Geophys. J. R. astr. Soc. (1985) **80**, 121–147

Kirchhoff–Helmholtz reflection seismograms in a laterally inhomogeneous multi-layered elastic medium – I. Theory

L. Neil Frazer and Mrinal K. Sen *Hawaii Institute of Geophysics, University of Hawaii at Manoa, Honolulu, Hawaii 96822, USA*

Received 1984 July 2; in original form 1984 January 27

Summary. In a medium consisting of elastic layers with irregular interfaces, Kirchhoff–Helmholtz (KH) theory can be extended to synthesize the motion due to various generalized rays. An exact elastic form of the KH integral is first derived, then various asymptotic approximations are used to convert this integral into one which can be rapidly evaluated to give the motion of a single generalized ray. The approximations used are those of geometrical optics, for propagation across layers, and the Kirchhoff or tangent-plane approximation for propagation across boundaries. It is shown how the KH method leads naturally to a generalization of our usual notion of elastic reflection and transmission coefficients. The new coefficients are functions of both angle of incidence and angle of reflection or transmission and they are derived so as to obtain coordinate-free formulae that show clearly their relation to the conventional Snell's law coefficients. The elastic KH method is applied first to the problem of a single interface, where its performance is compared to that of the Gaussian beam and Maslov methods. (For synthesizing reflections from irregular interfaces the KH method is superior because it includes signals diffracted from corners. However, when the interface is very smooth on the scale of a wavelength the Maslov and Gaussian beam methods are superior because they do not break down when there is a caustic on the reflector.) KH theory is then applied to a multilayered elastic medium and it is shown how the effects of frequency-dependent attenuation and dispersion can be incorporated into the theory by taking advantage of the approximately logarithmic variation of slowness with frequency in most earth materials. The limitations of the KH theory are discussed and some recent attempts to overcome these difficulties are reviewed. A new method for overcoming the problem of a caustic on the reflector becomes apparent when the KH integral is regarded as a member of a larger family of equivalent 1-fold integrals all of which are derivable from the same multifold path integral. Refracted or diving rays can be treated within the same formalism with equal benefit. For velocity models that are independent of one spatial direction (strike) a method is given for approximately converting 2-D results into 3-D results.

1 Introduction

The Kirchhoff–Helmholtz (KH) integral (Helmholtz 1860; Kirchhoff 1883) has been applied to many problems in wave propagation. Mow & Pao (1971) review its application in the diffraction of elastic waves by cylinders and spheres. Burridge (1962, 1963) used it to calculate reflections in liquid and solid spheres and recently Haddon & Buchen (1981) adapted Burridge's method to the synthesis of PKP. Scott & Helmberger (1983) used the KH integral to model body wave reflections from mountain topography and spall from nuclear blasts. Application of the method to the synthesis of finite frequency body wave synthetic seismograms in media with laterally inhomogeneous but continuous velocity was made by Sinton & Frazer (1981), Haddon (1982), Zherniak (1983), and Frazer & Sinton (1984).

In exploration seismology Hilterman (1970, 1975, 1982), Trorey (1970, 1977) and Berryhill (1977) have used the KH technique to model small offset reflection data for reflecting surfaces embedded in a homogeneous acoustic half-space. Extensions of these methods to the case of a laterally varying velocity were given by Hilterman & Larsen (1975), Berryhill (1979), Carter & Frazer (1983), and Deregowski & Brown (1983).

The elastodynamic form of the KH integral (Love 1904, 1944; de Hoop 1958; Wheeler & Sternberg 1968) has been applied to the calculation of reflected wavefields less often than the acoustic form. Until recently most reflection data were gathered with small lateral separation of sources and receivers so that very little conversion of compressional energy to shear energy occurred and losses due to mode conversion could be neglected. Also sources and receivers were designed to enhance compressional energy at the expense of shear wave energy. In this paper we are interested in wide angle reflections as well as near vertical reflections so that (even when shear wave arrivals are not computed) the loss in amplitude and change in phase of compressional arrivals due to shear conversion must be accounted for.

A derivation of the time domain form of the elastodynamic Kirchhoff integral can be found in Aki & Richards (1980). For completeness we include here a brief derivation of the frequency domain form of the integral that will be needed in the sequel. As shown in Fig. 1 let V be an open volume in a 2- or 3-D elastic medium and let ∂V be the boundary of V with outward pointing unit normal $\hat{\mathbf{n}}$. Let $\mathbf{f}_1$ be some distribution of body force density which vanishes on V and ∂V, and let $\mathbf{u}_1$ and $\boldsymbol{\tau}_1$ be the displacement and stress associated with $\mathbf{f}_1$ so that these quantities satisfy the frequency domain momentum equation $-\rho\omega^2\mathbf{u}_1 = \nabla\cdot\boldsymbol{\tau}_1 + \mathbf{f}_1$. Also, let $\mathbf{f}_2$ be some distribution of body force which vanishes both outside V and on ∂V and let $\mathbf{u}_2$ and $\boldsymbol{\tau}_2$ be the displacement and

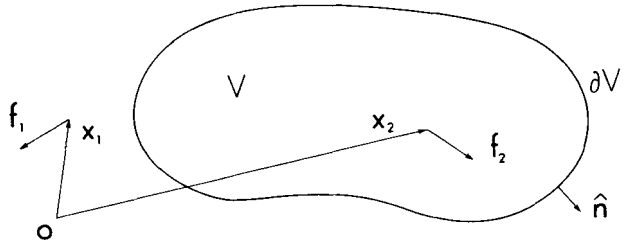

Figure 1. A volume V in (E^2 or E^3) with boundary ∂V. The vector $\hat{\mathbf{n}}$ is the outward-pointing unit normal to ∂V. We wish to calculate the displacement at $\mathbf{x}_2$ due to a force $\mathbf{f}_1$ at $\mathbf{x}_1$.

stress associated with $\mathbf{f}_2$, so that $-\rho\omega^2\mathbf{u}_2 = \nabla\cdot\boldsymbol{\tau}_2 + \mathbf{f}_2$. Using the divergence theorem we write

$$\int_{\partial V} \hat{\mathbf{n}}\cdot(\boldsymbol{\tau}_1\cdot\mathbf{u}_2 - \boldsymbol{\tau}_2\cdot\mathbf{u}_1)\,dA = \int_V \nabla\cdot(\boldsymbol{\tau}_1\cdot\mathbf{u}_2 - \boldsymbol{\tau}_2\cdot\mathbf{u}_1)\,dV. \tag{1}$$

However, for any vector $\mathbf{u}$ and second-order tensor $\boldsymbol{\tau}$, $\nabla\cdot(\boldsymbol{\tau}\cdot\mathbf{u}) = (\nabla\cdot\boldsymbol{\tau})\cdot\mathbf{u} + \tau:\nabla\mathbf{u}$. (To interpret this last equation let $\{x^i\}_{i=1}^3$ be any system of coordinates for E^3. Then $\nabla = \nabla x^i\partial/\partial x^i$ and $\boldsymbol{\tau}:\nabla\mathbf{u} = \nabla x^i\cdot\boldsymbol{\tau}\cdot\partial_i\mathbf{u}$ – e.g. Backus 1967.) Thus the integral on the right side of (1) becomes

$$\int_V [(\nabla\cdot\boldsymbol{\tau}_1)\cdot\mathbf{u}_2 - (\nabla\cdot\boldsymbol{\tau}_2)\cdot\mathbf{u}_1 + \boldsymbol{\tau}_1:\nabla\mathbf{u}_2 - \boldsymbol{\tau}_2:\nabla\mathbf{u}_1]\,dV. \tag{2}$$

But $\boldsymbol{\tau}_1$ and $\mathbf{u}_1$ are related by the fourth-order elastic tensor $\boldsymbol{c}$ and because of the symmetries of $\boldsymbol{c}$ we have $\boldsymbol{\tau}_1:\nabla\mathbf{u}_2 = (\boldsymbol{c}:\nabla\mathbf{u}_1):\nabla\mathbf{u}_2 = \nabla\mathbf{u}_1:\boldsymbol{c}:\nabla\mathbf{u}_2 = \nabla\mathbf{u}_2:\boldsymbol{c}:\nabla\mathbf{u}_1 = \boldsymbol{\tau}_2:\nabla\mathbf{u}_1$. Thus the last two terms in the integral (2) cancel each other. In the remainder of (2) we replace $\nabla\cdot\boldsymbol{\tau}_1$ by $-\rho\omega^2\mathbf{u}_1 - \mathbf{f}_1$ and $\nabla\cdot\boldsymbol{\tau}_2$ by $-\rho\omega^2\mathbf{u}_2 - \mathbf{f}_2$, respectively. Since $\mathbf{f}_1$ vanishes on V and ∂V the integral (2) reduces to $\int_V \mathbf{f}_2\cdot\mathbf{u}_1\,dV$. To summarize, we have shown that if $\mathbf{f}_1$ vanishes on V and ∂V, and if $\mathbf{f}_2$ vanishes outside V and on ∂V, then

$$\int_V \mathbf{f}_2\cdot\mathbf{u}_1\,dV = \int_{\partial V}\hat{\mathbf{n}}\cdot(\boldsymbol{\tau}_1\cdot\mathbf{u}_2 - \boldsymbol{\tau}_2\cdot\mathbf{u}_1)\,dA. \tag{3}$$

When this relation is used for calculations the fictitious force $\mathbf{f}_2$ is chosen in accordance with the nature of the actual receiver located at $\mathbf{x}_2$. If there is a pressure sensor at $\mathbf{x}_2$ then choosing $\mathbf{f}_2 = \nabla\delta(\mathbf{x} - \mathbf{x}_2)$ and using the fact that $\mathbf{x}_2$ is an interior point of V we may write

$$\begin{aligned}\int_V \mathbf{f}_2\cdot\mathbf{u}_1\,dV &= \int_V \mathbf{u}_1\cdot\nabla\delta(\mathbf{x} - \mathbf{x}_2)\,dV \\ &= \int_V \nabla\cdot\{\delta(\mathbf{x} - \mathbf{x}_2)\,\mathbf{u}_1\}\,dV - \int_V \delta(\mathbf{x} - \mathbf{x}_2)\;\nabla\cdot\mathbf{u}_1\,dV \\ &= -\nabla\cdot\mathbf{u}_1(\mathbf{x}_2).\end{aligned}$$

Then since pressure P is given by $-k\nabla\cdot\mathbf{u}$ where k is bulk modulus, the pressure field at $\mathbf{x}_2$ due to $\mathbf{f}_1$ is

$$P_1(\mathbf{x}_2) = k(\mathbf{x}_2)\int_{\partial V}\hat{\mathbf{n}}\cdot(\boldsymbol{\tau}_1\cdot\mathbf{u}_2 - \boldsymbol{\tau}_2\cdot\mathbf{u}_1)\,dA. \tag{4}$$

If the detector at $\mathbf{x}_2$ meaures motion in the direction $\hat{\mathbf{a}}_2$ then choosing $\mathbf{f}_2 = \hat{\mathbf{a}}_2\,\delta(\mathbf{x} - \mathbf{x}_2)$ yields

$$\int_V \mathbf{f}_2\cdot\mathbf{u}_1\,dV = \int_V \delta(\mathbf{x} - \mathbf{x}_2)\,\mathbf{a}_2\cdot\mathbf{u}_1\,dV = \mathbf{a}_2\cdot\mathbf{u}_1(\mathbf{x}_2)$$

and so

$$\mathbf{a}_2\cdot\mathbf{u}_1(\mathbf{x}_2) = \int_{\partial V}\hat{\mathbf{n}}\cdot(\boldsymbol{\tau}_1\cdot\mathbf{u}_2 - \boldsymbol{\tau}_2\cdot\mathbf{u}_1)\,dA. \tag{5}$$

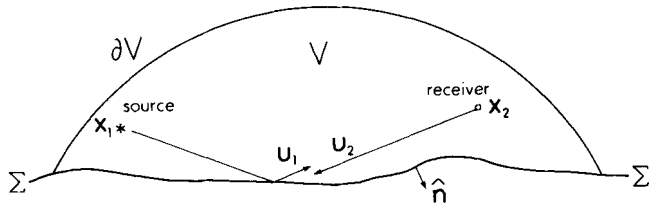

Figure 2. Application of the KH equations (4) and (5) to the calculation of waves reflected from a material discontinuity Σ. As $\mathbf{u}_1$ is a reflected field it appears to originate from sources outside V.

In the sequel we will also use these formulae to calculate energy reflected from a material discontinuity which coincides with a part of the surface of integration as shown in Fig. 2. Here the volume V contains both $\mathbf{x}_1$ and $\mathbf{x}_2$; however, at each point on the scattering surface Σ the quantity $\mathbf{u}_1$ in (4) and (5) is the *reflected P-* (or *S-*) wavefield, which appears to emanate from points outside of V. Thus, although the physical source point is inside V, the virtual source region is not, and so none of the assumptions used in the derivation above are violated. In Fig. 2 the reflected field $\mathbf{u}_1$ does not vanish on $\partial V \backslash \Sigma$. However, since $\partial V \backslash \Sigma$ is very distant from $\mathbf{x}_2$ the contribution to $\mathbf{u}_1(\mathbf{x}_2)$ of the integral over $\partial V \backslash \Sigma$ arrives much later in time than the contribution from the integral over Σ. Thus the former may be neglected.

If the scattered field $\mathbf{u}_1$ and the incident field $\mathbf{u}_2$ are exactly known on ∂V then equations (4) and (5) hold exactly. However, the usefulness of these equations inheres in the fact that often $\mathbf{u}_1$ and $\mathbf{u}_2$ are easy to calculate on Σ whereas $\mathbf{u}_1(\mathbf{x}_2)$ may be difficult to calculate directly because of the presence of caustics or multiple arrivals. In such circumstances equation (5) can be an efficient method of computing $\mathbf{u}_1(\mathbf{x}_2)$.

2 Plane wave theory

In Section 4 we will use equation (5) to derive formulae for the motion due to various kinds of generalized rays in 2- and 3-D models. These formulae will have the property that they give the geometrical optics solution for $\mathbf{u}_1(\mathbf{x}_2)$ whenever geometrical optics are valid but that, in addition, they also give a correct solution when $\mathbf{x}_2$ is located on a caustic of the $\mathbf{u}_1$ wavefield. To derive these formulae we assume that the length scale of the variation in Σ is much greater than the wavelength of the signal. Thus near Σ we may treat both $\mathbf{u}_1$ and $\mathbf{u}_2$ as if they were plane waves. To obtain the stress fields associated with these waves we use the constitutive relation $\boldsymbol{\tau} = \lambda \nabla \cdot \mathbf{u}\, \mathbf{I} + \mu [\nabla \mathbf{u} + (\nabla \mathbf{u})^{\mathrm{T}}]$ in which λ and μ are Lamé parameters and $\mathbf{I}$ is the identity tensor in E^3. For a P-wave with displacement $\mathbf{u}^P$, local direction of propagation $\hat{\mathbf{t}}^P$, amplitude A and local P-wave speed α we have

$$\mathbf{u}^P = A\hat{\mathbf{t}}^P \exp\{i\omega(\hat{\mathbf{t}}^P \cdot \mathbf{r})/\alpha\},$$

$$\nabla \mathbf{u}^P = \frac{i\omega}{\alpha} \hat{\mathbf{t}}^P \mathbf{u}^P,$$

$$\nabla \cdot \mathbf{u}^P = \frac{i\omega}{\alpha} \mathbf{u}^P \cdot \hat{\mathbf{t}}^P$$

and

$$\boldsymbol{\tau}^P = \frac{i\omega}{\alpha} \{\lambda(\mathbf{u}^P \cdot \hat{\mathbf{t}}^P)\, \mathbf{I} + 2\mu\, \mathbf{u}^P \hat{\mathbf{t}}^P\}. \tag{6}$$

For an S-wave with displacement $\mathbf{u}^S$, local direction of propagation $\hat{\mathbf{t}}^S$, amplitude $\mathbf{A}$ and local S-wave speed β we have $\mathbf{u}^S = \mathbf{A}\exp\{i\omega(\mathbf{t}^S\cdot\mathbf{r})/\beta\}$where $\hat{\mathbf{t}}^S\cdot\mathbf{A}=0$, $\nabla\mathbf{u}^S=(i\omega/\beta)\hat{\mathbf{t}}^S\mathbf{u}^S$, $\nabla\cdot\mathbf{u}^S=0$ and

$$\boldsymbol{\tau}^S=\frac{i\omega}{\beta}\mu(\hat{\mathbf{t}}^S\mathbf{u}^S+\mathbf{u}^S\hat{\mathbf{t}}^S). \tag{7}$$

Then for two P-waves, $\mathbf{u}_A^P$ and $\mathbf{u}_B^P$, the integral of (5), henceforth referred to as the P interaction, is

$$\hat{\mathbf{n}}\cdot(\boldsymbol{\tau}_A^P\cdot\mathbf{u}_B^P-\boldsymbol{\tau}_B^P\cdot\mathbf{u}_A^P)=\frac{i\omega}{\alpha}\mathbf{u}_A^P\cdot\{\lambda(\hat{\mathbf{t}}_A^P\hat{\mathbf{n}}-\hat{\mathbf{n}}\hat{\mathbf{t}}_B^P)+2\mu(\hat{\mathbf{n}}\hat{\mathbf{t}}_A^P-\hat{\mathbf{t}}_B^P\hat{\mathbf{n}})\}\cdot\mathbf{u}_B^P \tag{8a}$$

and for two S-waves, $\mathbf{u}_A^S$ and $\mathbf{u}_B^S$, the S interaction is

$$\mathbf{n}\cdot(\boldsymbol{\tau}_A^S\cdot\mathbf{u}_B^S-\boldsymbol{\tau}_B^S\cdot\mathbf{u}_A^S)=\frac{i\omega}{\beta}\mu\mathbf{u}_A^S\cdot\{\hat{\mathbf{n}}\cdot(\hat{\mathbf{t}}_A^S-\hat{\mathbf{t}}_B^S)\,\mathsf{I}+(\hat{\mathbf{n}}\hat{\mathbf{t}}_A^S-\hat{\mathbf{t}}_B^S\hat{\mathbf{n}})\}\cdot\mathbf{u}_B^S. \tag{8b}$$

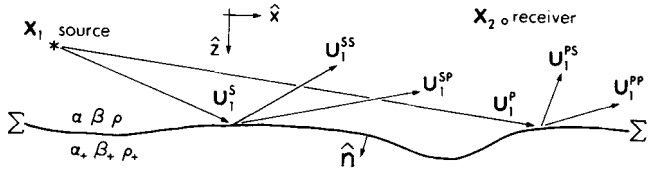

Figure 3. Two elastic half-spaces welded together along an irregular boundary.

In our use of equation (8) $\mathbf{u}_A$ will generally be a reflected wavefield of the kind shown in Fig. 3. We will use $\mathbf{u}_1^P$ and $\mathbf{u}_1^S$ to denote the P- and S-waves radiated by the source at $\mathbf{x}_1$. The P- and S-wave reflections of $\mathbf{u}_1^P$ from Σ will be denoted $\mathbf{u}_1^{PP}$ and $\mathbf{u}_1^{PS}$, respectively and the P- and S-wave reflections of $\mathbf{u}_1^S$ will be denoted $\mathbf{u}_1^{SP}$ and $\mathbf{u}_1^{SS}$, respectively. The reflected fields are obtained from the incident field by use of the invariant plane wave reflection formulae given in Appendix 1. For example let $\mathbf{u}_1^{PP}=A_1^{PP}\hat{\mathbf{t}}_1^{PP}$ be the P-wave reflected by Σ from $\mathbf{u}_1^P=A_1^P\hat{\mathbf{t}}_1^P$. Then $\mathbf{u}_1^{PP}=\mathbf{u}_1^P\cdot\hat{\mathbf{t}}_1^P\grave{P}\acute{P}\hat{\mathbf{t}}_1^{PP}$ in which $\grave{P}\acute{P}$ is one of the plane wave coefficients of Aki & Richards (1980) and $\hat{\mathbf{t}}_1^{PP}=\hat{\mathbf{t}}_1^P\cdot(\mathsf{I}-2\hat{\mathbf{n}}\hat{\mathbf{n}})$ where $\hat{\mathbf{n}}$ is the local normal to Σ. We can use this relation to write the P interaction for $\mathbf{u}_1^{PP}$ and $\mathbf{u}_2^P$ in terms of $\mathbf{u}_1^P$ and $\mathbf{u}_2^P$. Thus we obtain the PP interaction

$$\hat{\mathbf{n}}\cdot(\boldsymbol{\tau}_1^{PP}\cdot\mathbf{u}_2^P-\boldsymbol{\tau}_2^P\cdot\mathbf{u}_1^{PP})=\mathbf{u}_1^{PP}\cdot\mathsf{R}_{12}^{PP}\cdot\mathbf{u}_2^P; \tag{9a}$$

$$\mathsf{R}_{12}^{PP}=\hat{\mathbf{t}}_1^P\grave{P}\acute{P}\frac{i\omega}{\alpha}\hat{\mathbf{t}}_1^{PP}\cdot\{\lambda(\hat{\mathbf{t}}_1^{PP}\hat{\mathbf{n}}-\hat{\mathbf{n}}\hat{\mathbf{t}}_2^P)+2\mu(\hat{\mathbf{n}}\hat{\mathbf{t}}_1^{PP}-\hat{\mathbf{t}}_2^P\hat{\mathbf{n}})\} \tag{9b}$$

in which

$$\hat{\mathbf{t}}_1^{PP}=\hat{\mathbf{t}}_1^P\cdot(\mathsf{I}-2\hat{\mathbf{n}}\hat{\mathbf{n}}). \tag{9c}$$

Similarly for $\mathbf{u}_1^{PS}$ and $\mathbf{u}_2^S$ we have the PS interaction

$$\hat{\mathbf{n}}\cdot(\boldsymbol{\tau}_1^{PS}\cdot\mathbf{u}_2^S-\boldsymbol{\tau}_2^S\cdot\mathbf{u}_1^{PS})=\mathbf{u}_1^P\cdot\mathsf{R}_{12}^{PS}\cdot\mathbf{u}_2^S; \tag{10a}$$

$$\mathsf{R}_{12}^{PS}=\hat{\mathbf{t}}_1^P\grave{P}\acute{V}\left(\frac{i\omega}{\beta}\right)\mu\hat{\boldsymbol{\psi}}_1^{PS}\cdot\{\hat{\mathbf{n}}\cdot(\hat{\mathbf{t}}_1^{PS}-\hat{\mathbf{t}}_2^S)\,\mathsf{I}+(\hat{\mathbf{n}}\hat{\mathbf{t}}_1^{PS}-\hat{\mathbf{t}}_2^S\hat{\mathbf{n}})\} \tag{10b}$$

in which

$$\hat{\boldsymbol{\nu}}_1^{PS} = \hat{\mathbf{t}}_1^{PS} \cdot (\hat{\boldsymbol{\sigma}}\hat{\mathbf{n}} - \hat{\mathbf{n}}\hat{\boldsymbol{\sigma}});$$

$$\hat{\mathbf{t}}_1^{PS} = \beta\sigma\hat{\boldsymbol{\sigma}} - \sqrt{1-\beta^2\sigma^2}\,\hat{\mathbf{n}}, \qquad \mathrm{Im}(\surd) \geqslant 0; \tag{10c, d}$$

$$\boldsymbol{\sigma} = \hat{\mathbf{t}}_1^{P} \cdot (\mathbf{I} - \hat{\mathbf{n}}\hat{\mathbf{n}})/\alpha;\ \sigma = ||\,\boldsymbol{\sigma}\,||;\ \hat{\boldsymbol{\sigma}} = \boldsymbol{\sigma}/\sigma. \tag{10e, f, g}$$

For $\mathbf{u}_1^{SP}$ and $\mathbf{u}_2^{P}$ we obtain the *SP* interaction

$$\hat{\mathbf{n}} \cdot (\boldsymbol{\tau}_1^{SP} \cdot \mathbf{u}_2^{P} - \boldsymbol{\tau}_2^{P} \cdot \mathbf{u}_1^{SP}) = \mathbf{u}_1^{S} \cdot \mathsf{R}_{12}^{SP} \cdot \mathbf{u}_2^{P} \tag{11a}$$

$$\mathsf{R}_{12}^{SP} = \hat{\boldsymbol{\nu}}_1^{S}\grave{V}\acute{P}\left(\frac{i\omega}{\alpha}\right)\mathbf{t}_1^{SP} \cdot \{\lambda(\hat{\mathbf{t}}_1^{SP}\hat{\mathbf{n}} - \hat{\mathbf{n}}\hat{\mathbf{t}}_2^{P}) + 2\mu(\hat{\mathbf{n}}\hat{\mathbf{t}}_1^{SP} - \hat{\mathbf{t}}_2^{P}\hat{\mathbf{n}})\} \tag{11b}$$

in which

$$\hat{\boldsymbol{\nu}}_1^{S} = \hat{\mathbf{t}}_1^{S} \cdot (\hat{\mathbf{n}}\hat{\boldsymbol{\sigma}} - \hat{\boldsymbol{\sigma}}\hat{\mathbf{n}});$$

$$\hat{\mathbf{t}}_1^{SP} = \alpha\sigma\hat{\boldsymbol{\sigma}} - \sqrt{1-\alpha^2\sigma^2}\,\hat{\mathbf{n}}, \qquad \mathrm{Im}(\surd) \geqslant 0; \tag{11c, d}$$

$$\boldsymbol{\sigma} = \hat{\mathbf{t}}_1^{S} \cdot (\mathbf{I} - \hat{\mathbf{n}}\hat{\mathbf{n}})/\beta;\ \sigma = ||\,\boldsymbol{\sigma}||;\ \hat{\boldsymbol{\sigma}} = \boldsymbol{\sigma}/\sigma. \tag{11e, f, g}$$

And for $\mathbf{u}_1^{SS}$ and $\mathbf{u}_2^{SS}$ we obtain the *SS* interaction

$$\hat{\mathbf{n}} \cdot (\boldsymbol{\tau}_1^{SS} \cdot \mathbf{u}_2^{S} - \boldsymbol{\tau}_2^{S} \cdot \mathbf{u}_1^{SS}) = \mathbf{u}_1^{S} \cdot \mathsf{R}_{12}^{SS} \cdot \mathbf{u}_2^{S} \tag{12a}$$

$$\mathsf{R}_{12}^{SS} = (\hat{\boldsymbol{\nu}}_1^{S}\grave{V}\acute{V}\hat{\boldsymbol{\nu}}_1^{SS} + \hat{\boldsymbol{\eta}}\grave{H}\acute{H}\hat{\boldsymbol{\eta}}) \cdot \frac{i\omega}{\beta}\mu\,\{\hat{\mathbf{n}} \cdot (\hat{\mathbf{t}}_1^{SS} - \hat{\mathbf{t}}_2^{S})\,\mathbf{I} + (\hat{\mathbf{n}}\hat{\mathbf{t}}_1^{SS} - \hat{\mathbf{t}}_2^{S}\hat{\mathbf{n}})\} \tag{12b}$$

in which

$$\hat{\boldsymbol{\nu}}_1^{S} = \mathbf{t}_1^{S} \cdot (\hat{\mathbf{n}}\hat{\boldsymbol{\sigma}} - \hat{\boldsymbol{\sigma}}\hat{\mathbf{n}});\ \hat{\mathbf{t}}_1^{SS} = \hat{\mathbf{t}}_1^{S} \cdot (\mathbf{I} - 2\hat{\mathbf{n}}\hat{\mathbf{n}});\ \hat{\boldsymbol{\nu}}_1^{SS} = \hat{\boldsymbol{\nu}}_1^{S} \cdot (\mathbf{I} - 2\hat{\mathbf{n}}\hat{\mathbf{n}}) \tag{12c, d, e}$$

$$\boldsymbol{\sigma} = \mathbf{t}_1^{S} \cdot (\mathbf{I} - \hat{\mathbf{n}}\hat{\mathbf{n}})/\beta;\ \hat{\boldsymbol{\sigma}} = \boldsymbol{\sigma}/||\,\boldsymbol{\sigma}\,|| \tag{12f, g}$$

$$\hat{\boldsymbol{\eta}} = (\hat{\mathbf{t}}_1^{S} \times \hat{\mathbf{n}})/||\,\hat{\mathbf{t}}_1^{S} \times \hat{\mathbf{n}}\,||. \tag{12h}$$

The quantities R_{12}^{PP}, R_{12}^{PS}, R_{12}^{SP}, R_{12}^{SS} will be referred to as *interaction coefficients*, or elastic Kirchhoff–Helmholtz reflection coefficients. Note that with these definitions R_{12}^{PP} is a function of $\hat{\mathbf{t}}_1^{P}$, $\hat{\mathbf{t}}_2^{P}$ and $\hat{\mathbf{n}}$, R_{12}^{PS} is a function of $\hat{\mathbf{t}}_1^{P}$, $\hat{\mathbf{t}}_2^{S}$ and $\hat{\mathbf{n}}$, R_{12}^{SP} is a function of $\hat{\mathbf{t}}_1^{S}$, $\hat{\mathbf{t}}_2^{P}$ and $\hat{\mathbf{n}}$, and R_{12}^{SS} is a function of $\hat{\mathbf{t}}_1^{S}$, $\hat{\mathbf{t}}_2^{S}$ and $\hat{\mathbf{n}}$. These definitions are completely coordinate-free so that to apply them in any particular coordinate system one needs only to have a formula for the dot product in that system. However, it should be emphasized that these interaction coefficients are asymptotic, being correct only at high frequencies where the radii of curvature of Σ are much larger than a wavelength of the signal. They give only the effect of a single interaction of the incident field with Σ. Phenomena such as head waves, which involve multiple interactions with the surface, are not included.

3 Results from geometrical optics

In geometrical optics (Babich & Alekseev 1958; Karal & Keller 1959) one obtains the radiation field of a point source by tracing rays, to obtain travel times; and by assuming

that energy flux is conserved along ray tubes, to obtain amplitudes. We omit the derivations of the geometrical optics formulae as these can be found in many books and papers (e.g. Červený, Molotkov & Pšenčík 1977; Aki & Richards 1980; Frazer & Phinney 1980).

Consider first the problem of an elastic medium with a point source located at $\mathbf{x}_1$. We assume that α, β and ρ are smooth functions of spatial position and that the wavelength of the signal is small compared to the scale length of the variations in these parameters. Then the *P*-wave motion $\mathbf{u}_1^P$ and *S*-wave motion $\mathbf{u}_1^S$ propagate independently and we have for the motions in a 2- or 3-D medium

$$\mathbf{u}_1^P(\mathbf{x}) \simeq \frac{\hat{\mathbf{t}}_1^P F_1^P \exp(i\omega T_1^P)}{\sqrt{\rho\alpha\rho_1\alpha_1}\, B_1^P} \tag{13}$$

and

$$\mathbf{u}_1^S(\mathbf{x}) \simeq \frac{(\hat{\mathbf{b}}_1 F_1^b + \hat{\mathbf{c}}_1 F_1^c)\exp(i\omega T_1^S)}{\sqrt{\rho\beta\rho_1\beta_1}\, B_1^S}. \tag{14}$$

In equation (13) $\hat{\mathbf{t}}_1^P = \hat{\mathbf{t}}_1^P(\mathbf{x}, \mathbf{x}_1)$ is the tangent at $\mathbf{x}$ to the *P*-ray from $\mathbf{x}_1$ to $\mathbf{x}$, and $T_1^P = T^P(\mathbf{x}, \mathbf{x}_1)$ is the *P*-wave travel time from $\mathbf{x}_1$ to $\mathbf{x}$. In the denominator the densities are $\rho = \rho(\mathbf{x})$ and $\rho_1 = \rho(\mathbf{x}_1)$ and the *P*-wave velocities are $\alpha = \alpha(\mathbf{x})$ and $\alpha_1 = \alpha(\mathbf{x}_1)$. The source term $F_1^P = F^P(\mathbf{x}, \mathbf{x}_1)$ and spreading factor $B_1^P = B^P(\mathbf{x}, \mathbf{x}_1)$ are discussed in detail below. The unit vectors $\hat{\mathbf{b}}_1 = \hat{\mathbf{b}}(\mathbf{x}, \mathbf{x}_1)$ and $\hat{\mathbf{c}}_1 = \hat{\mathbf{c}}(\mathbf{x}, \mathbf{x}_1)$ shown in Fig. 4(c) are normal to each other and normal to the unit vector $\hat{\mathbf{t}}_1^S = \hat{\mathbf{t}}^S(\mathbf{x}, \mathbf{x}_1)$ which is tangent at $\mathbf{x}$ to the *S*-ray from $\mathbf{x}_1$ to $\mathbf{x}$. The vectors $\{\hat{\mathbf{t}}_1^S, \hat{\mathbf{b}}_1, \hat{\mathbf{c}}_1\}$ are a frame field on the *S*-ray. Thus for rays in a 3-D medium $\hat{\mathbf{b}}_1$ and $\hat{\mathbf{c}}_1$ rotate about $\mathbf{t}_1$ at a rate equal to the torsion of the ray. In the numerator of (14) $F_1^b = F_1^b(\mathbf{x}, \mathbf{x}_1)$ and $F_1^c = F_1^c(\mathbf{x}, \mathbf{x}_1)$ are source terms, and in the denominator $B_1^S = B_1^S(\mathbf{x}, \mathbf{x}_1)$ is a spreading factor.

In a 3-D medium the spreading factors are

$$B_1^P = 4\pi\alpha_1\sqrt{dA/d\Omega} \quad \text{and} \quad B_1^S = 4\pi\beta_1\sqrt{dA/d\Omega} \tag{15a, b}$$

where, as shown in Fig. 4(a), dA is the cross-sectional area at $\mathbf{x}$ of the ray tube which subtends solid angle $d\Omega$ at the source. Since the ray tube for the *P*-wave will in general be different from that of the *S*-wave, $dA/d\Omega$ refers to the *P*-wave in (15a) and to the *S*-wave in (15b). In a homogeneous medium $\sqrt{dA/d\Omega} = \|\mathbf{x} - \mathbf{x}_1\|$ for both *P* and *S*. In a 2-D medium the spreading factors are

$$B_1^P = \sqrt{8\pi\omega\alpha_1\, dl/d\theta}\exp(-i\pi/4) \quad \text{and} \quad B_1^S = \sqrt{8\pi\omega\beta_1\, dl/d\theta}\exp(-i\pi/4) \tag{16a, b}$$

where as shown in Fig. 4(b) dl is the cross-sectional width of the ray tube which subtends an angle $d\theta$ at the source. Again $dl/d\theta$ is in general different for *P*- and *S*-waves. However, in a homogeneous medium $dl/d\theta = \|\mathbf{x} - \mathbf{x}_1\|$ for both *P* and *S*. The quantities $dA/d\Omega$ and $dl/d\theta$ can be calculated either by integration of the ray equations (e.g. Červený & Hron

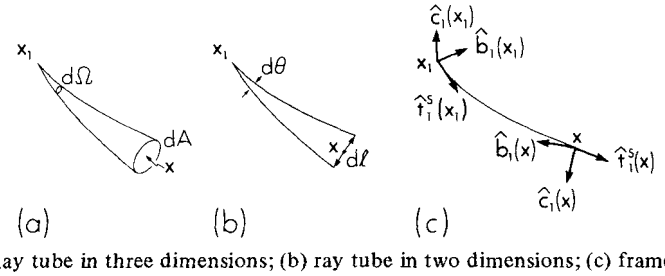

Figure 4. (a) Ray tube in three dimensions; (b) ray tube in two dimensions; (c) frame field on a ray.

1980) or by numerical differencing (e.g. Sinton & Frazer 1982). An approximate method for converting 2-D solutions into 3-D solutions is given in Appendix B.

Equations (15a, b) and (16a, b) assume that the ray between $\mathbf{x}_1$ and $\mathbf{x}$ has encountered no caustics. If in fact the ray has encountered one or more caustics then B must be multiplied by $\exp\{-i\,\mathrm{sgn}(\omega)\,\sigma(\mathbf{x}, \mathbf{x}_1)\,\pi/2\}$ where $\sigma(\mathbf{x}, \mathbf{x}_1)$ is the KMAH index (Ziolkowski & Deschamps 1980). Here we need only remember that for 2-D problems the KMAH index of a ray is initially zero and increases by 1 every time the ray encounters a caustic.

In equations (13) and (14) the form of the terms F^P, F^b and F^c depends on the nature of the source. For a point force the equivalent body force density (Burridge & Knopoff 1964) is $\mathbf{f}_1 = \mathbf{a}(\omega)\,\delta(\mathbf{x} - \mathbf{x}_1)$ and we have

$$F_1^P = \mathbf{a} \cdot \mathbf{t}_1^P(\mathbf{x}_1);\ F_1^b = \mathbf{a} \cdot \mathbf{b}_1(\mathbf{x}_1);\ F_1^c = \mathbf{a} \cdot \mathbf{c}_1(\mathbf{x}_1). \tag{17a, b, c}$$

In these relations $\hat{\mathbf{t}}_1^P(\mathbf{x}_1)$ is the tangent at the source $\mathbf{x}_1$ to the P-ray from $\mathbf{x}_1$ to $\mathbf{x}$. Similarly $\hat{\mathbf{b}}_1(\mathbf{x}_1)$ and $\hat{\mathbf{c}}_1(\mathbf{x}_1)$ are the normals to the S-ray from $\mathbf{x}_1$ to $\mathbf{x}$, evaluated at $\mathbf{x}_1$. For a point double couple the equivalent body force density is $\mathbf{f}_1 = \mathsf{M} \cdot \nabla\delta(\mathbf{x} - \mathbf{x}_1)$ where $\mathsf{M} = \mathsf{M}(\omega)$ is the second-order symmetric moment tensor, and we have

$$F_1^P = \frac{i\omega}{\alpha_1}\hat{\mathbf{t}}_1^P(\mathbf{x}_1) \cdot \mathsf{M} \cdot \hat{\mathbf{t}}_1^P(\mathbf{x}_1) \tag{18a}$$

$$F_1^b = \frac{i\omega}{\beta_1}\hat{\mathbf{b}}_1(\mathbf{x}_1) \cdot \mathsf{M} \cdot \hat{\mathbf{t}}_1^S(\mathbf{x}_1) \tag{18b}$$

$$F_1^c = \frac{i\omega}{\beta_1}\hat{\mathbf{c}}_1(\mathbf{x}_1) \cdot \mathsf{M} \cdot \hat{\mathbf{t}}_1^S(\mathbf{x}_1). \tag{18c}$$

For a point explosion $\mathbf{f}_1 = P(\omega)\,\nabla\delta(\mathbf{x} - \mathbf{x}_1)$ and

$$F_1^P = \frac{i\omega}{\alpha_1}P(\omega);\ F_1^b = 0;\ F_1^c = 0. \tag{19a, b, c}$$

These last relations can be obtained from equations (18) by setting $\mathsf{M}(\omega) = P(\omega)\,\mathsf{I}$, where I is the identity tensor. Finally we note that for any travel-time function $T(\mathbf{x})$ we have $T(\mathbf{x}) = \hat{\mathbf{t}}(\mathbf{x})/v(\mathbf{x})$ where v is the local propagation speed and $\hat{\mathbf{t}}$ is the unit normal to the wavefront. Since pressure is $-\lambda\nabla \cdot \mathbf{u}$ the pressure field associated with equation (14) is zero and the pressure field associated with (13) is $(-i\omega\lambda/\alpha)F_1^P \exp(i\omega T_1^P)/(\sqrt{\rho\alpha\rho_1\alpha_1}\,B_1^P)$.

A scheme to obtain $dl/d\theta$ by numerical differencing is shown in Fig. 5. Let Σ be a line through the field point $\mathbf{x}$ and s denote distance along Σ. By shooting rays from $\mathbf{x}_1$ to Σ we

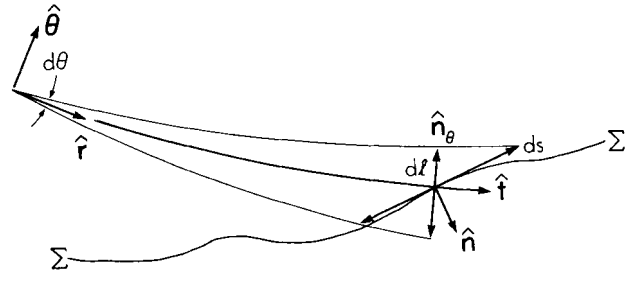

Figure 5. A differencing scheme for $dl/d\theta$. If s denotes distance along Σ then $dl/d\theta = \hat{\mathbf{n}} \cdot \hat{\mathbf{t}}\,ds/d\theta$. For the 3-D case see text.

obtain a function $s(\theta)$. If $\hat{\mathbf{n}}$ is the normal to Σ at $\mathbf{x}$ and $\hat{\mathbf{t}}$ is the unit tangent to the ray then

$$dl/d\theta = \hat{\mathbf{n}} \cdot \hat{\mathbf{t}}\, ds/d\theta. \tag{20}$$

In the 3-D case where Σ is a surface let s_1, s_2, be coordinates on Σ and $f(s_1, s_2)$ the function such that $dA = f(s_1, s_2)\, ds_1\, ds_2$ is an element of area on Σ. By shooting rays we get $s_1 = s_1(\theta, \phi)\, s_2 = s_2(\theta, \phi)$ where θ and ϕ are any spherical polar coordinates on the focal sphere Ω. Then

$$dA/d\Omega = \hat{\mathbf{n}} \cdot \hat{\mathbf{t}}\{(\partial s_1/\partial\theta)(\partial s_2/\partial\phi) - (\partial s_1/\partial\phi)(\partial s_2/\partial\theta)\}\, f\{s_1(\theta, \phi), s_2(\theta, \phi)\}/\sin\theta. \tag{21}$$

4 Reflected waves

4.1 A SINGLE INTERFACE

We are now in a position to write fairly simple expressions for the reflected wavefields from a surface Σ as shown in Fig. 3. In general, two inhomogeneous elastic media are in welded contact along Σ. We substitute (9a) into (5) to obtain $\mathbf{u}_1^{PP}$, the field of the *PP* reflection, and then use (13) to get $\mathbf{u}_1^P$ and $\mathbf{u}_2^P$ under the integral.

$$\mathbf{a}_2 \cdot \mathbf{u}_1^{PP}(\mathbf{x}_2) = \int_{\Sigma(\mathbf{x})} \mathbf{u}_1^P(\mathbf{x}) \cdot \mathsf{R}_{12}^{PP} \cdot \mathbf{u}_2^P(\mathbf{x})\, d\Sigma(\mathbf{x}) \tag{22a}$$

$$= \frac{1}{\sqrt{\rho_1\alpha_1\rho_2\alpha_2}} \int_{\Sigma(\mathbf{x})} \frac{F_1^P F_2^P}{\rho\alpha} \hat{\mathbf{t}}_1^P \cdot \mathsf{R}_{12}^{PP} \cdot \hat{\mathbf{t}}_2^P \frac{\exp[i\omega(T_1^P + T_2^P)]}{B_1^P B_2^P}\, d\Sigma(\mathbf{x}). \tag{22b}$$

In this expression F_1^P is one of the forms (17a), (18a) or (19a), depending on our choice of source, but $F_2^P = \mathbf{a}_2 \cdot \mathbf{t}_2^P(\mathbf{x}_2)$ where $\mathbf{t}_2^P$ is the unit tangent to the ray from $\mathbf{x}_2$ to $\mathbf{x}$, evaluated at $\mathbf{x}_2$ (our notation is as in Fig. 4c but with $\mathbf{x}_2$ instead of $\mathbf{x}_1$). Since both sides of (22) are linear in $\mathbf{a}_2$ we may suppress the factor '$\mathbf{a}_2$', and write just

$$\mathbf{u}_1^{PP}(\mathbf{x}_2) = \frac{1}{\sqrt{\rho_1\alpha_1\rho_2\alpha_2}} \int_{\Sigma(\mathbf{x})} \hat{\mathbf{t}}_2^P(\mathbf{x}_2) \frac{F_1^P}{\rho\alpha} \hat{\mathbf{t}}_1^P \cdot \mathsf{R}_{12}^{PP} \cdot \hat{\mathbf{t}}_2^P \frac{\exp[i\omega(T_1^P + T_2^P)]}{B_1^P B_2^P}\, d\Sigma(\mathbf{x}). \tag{23}$$

Let us review the meaning of each of the symbols in (23). Outside the integral sign we have $\rho_1 = \rho(\mathbf{x}_1)$, $\rho_2 = \rho(\mathbf{x}_2)$, $\alpha_1 = \alpha(\mathbf{x}_1)$, $\alpha_2 = \alpha(\mathbf{x}_2)$. Inside the integral sign $\hat{\mathbf{t}}_2^P(\mathbf{x}_2)$ is the tangent at $\mathbf{x}_2$ of the ray from $\mathbf{x}_2$ to $\mathbf{x}$. Thus $\hat{\mathbf{t}}_2^P(\mathbf{x}_2)$ is a function of $\mathbf{x}$ as well as $\mathbf{x}_2$. F_1^P is, as just noted, given by (17a), (18a), or (19a); in each of those equations there appears $\hat{\mathbf{t}}_1^P(\mathbf{x}_1)$ which is the tangent at $\mathbf{x}_1$ to the ray from $\mathbf{x}_1$ to $\mathbf{x}$. Thus $\hat{\mathbf{t}}_1^P(\mathbf{x}_1)$, and hence F_1^P, is a function of $\mathbf{x}$ as well as $\mathbf{x}_1$. The factor $\hat{\mathbf{t}}_1^P \cdot \mathsf{R}_{12}^{PP} \cdot \hat{\mathbf{t}}_2^P$ means $\hat{\mathbf{t}}_1^P(\mathbf{x}) \cdot \mathsf{R}_{12}^{PP} \cdot \hat{\mathbf{t}}_2^P(\mathbf{x})$ where R_{12}^{PP} is itself given as a function of $\hat{\mathbf{t}}_1^P(\mathbf{x})$, $\hat{\mathbf{t}}_2^P(\mathbf{x})$ and $\hat{\mathbf{n}}(\mathbf{x})$ by equations (9b, c), and $\hat{\mathbf{n}}(\mathbf{x})$ is the downward pointing unit normal to Σ at $\mathbf{x}$.

Note that ρ and α inside the integral in (23), and λ and μ in equation (9b) are evaluated *above* the interface Σ and these quantities may vary along Σ. The quantity $P\acute{P}$ in (9b) depends on velocities both above and below Σ and these too may vary. T_1^P and T_2^P are the *P*-wave travel times from $\mathbf{x}_1$ to $\mathbf{x}$ and from $\mathbf{x}_2$ to $\mathbf{x}$, respectively. If the integral is for three dimensions then according to equation (15a) $B_1^P = 4\pi\alpha_1\sqrt{dA_1(\mathbf{x})/d\Omega_1}$ and $B_2^P = 4\pi\alpha_2\sqrt{dA_2(\mathbf{x})/d\Omega_2}$. Here $dA_1(\mathbf{x})$ is the cross-sectional area at $\mathbf{x}$ of the ray tube which subtends solid angle $d\Omega_1$ at $\mathbf{x}_1$, and $dA_2(\mathbf{x})$ is the cross-sectional area at $\mathbf{x}$ of the ray tube which subtends solid angle $d\Omega_2$ at $\mathbf{x}_2$. Thus B_1^P and B_2^P can be obtained by shooting rays from

$\mathbf{x}_1$ and from $\mathbf{x}_2$ and differentiating according to equation (21). If the integral is for two dimensions then B_1^P is given by (16a) and B_2^P by a similar expression and these expressions can be obtained by differentiating according to equation (20). In two dimension $d\Sigma = ds$ where s is the curvilinear distance along Σ, but for three dimensions $d\Sigma = f(s_1, s_2)\, ds_1\, ds_2$ where f is a function and s_1 and s_2 are the coordinates for Σ introduced just before equation (21). Thus in either case $d\Sigma$ is the element of area on Σ.

To obtain an expression for the *PS* reflected wave we use relation (13) to get $\mathbf{u}_1^P$, relation (14) to get $\mathbf{u}_2^S$, and then substitute (10a) into (5) to obtain

$$\mathbf{u}_1^{PS}(\mathbf{x}_2) = \frac{1}{\sqrt{\rho_1\alpha_1\rho_2\beta_2}} \int_{\Sigma(\mathbf{x})} \frac{F_1^P}{\rho\sqrt{\alpha\beta}} \hat{\mathbf{t}}_1^P \cdot \mathsf{R}_{12}^{PS} \cdot \{\hat{\mathbf{b}}_2\hat{\mathbf{b}}_2(\mathbf{x}_2) + \hat{\mathbf{c}}_2\hat{\mathbf{c}}_2(\mathbf{x}_2)\} \times \frac{\exp[i\omega(T_1^P + T_2^S)]}{B_1^P B_2^S} d\Sigma(\mathbf{x}). \tag{24}$$

For the *SP* reflected wave, proceeding in a similar manner, we find

$$\mathbf{u}_1^{SP}(\mathbf{x}_2) = \frac{1}{\sqrt{\rho_1\beta_1\rho_2\alpha_2}} \int_{\Sigma(\mathbf{x})} \frac{(F_1^b\hat{\mathbf{b}}_1 + F_1^c\hat{\mathbf{c}}_1)}{\rho\sqrt{\alpha\beta}} \cdot \mathsf{R}_{12}^{SP} \cdot \hat{\mathbf{t}}_2\hat{\mathbf{t}}_2(\mathbf{x}_2) \frac{\exp[i\omega(T_1^S + T_2^P)]}{B_1^S B_2^P} d\Sigma(\mathbf{x}), \tag{25}$$

and for the *SS* reflected wave we get

$$\mathbf{u}_1^{SS}(\mathbf{x}_2) = \frac{1}{\sqrt{\rho_1\beta_1\rho_2\beta_2}} \int_{\Sigma(\mathbf{x})} \frac{(F_1^b\hat{\mathbf{b}}_1 + F_1^c\hat{\mathbf{c}}_1)}{\rho\beta} \cdot \mathsf{R}_{12}^{SS} \cdot \{\hat{\mathbf{b}}_2\hat{\mathbf{b}}_2(\mathbf{x}_2) + \hat{\mathbf{c}}_2\hat{\mathbf{c}}_2(\mathbf{x}_2)\} \times \frac{\exp[i\omega(T_1^S + T_2^S)]}{B_1^S B_2^S} d\Sigma(\mathbf{x}). \tag{26}$$

Here R_{12}^{SS}, for example, is well defined in terms of $\hat{\mathbf{t}}_1^S(\mathbf{x})$, $\hat{\mathbf{t}}_2^S(\mathbf{x})$ and $\hat{\mathbf{n}}(\mathbf{x})$ by relations (12b–h).

Equations (23)–(26) may be used when the surface Σ has corners or when the receiver is located at a caustic, but they contain the asymptotic interaction coefficients and so they give only the reflected field but not head waves or diving waves. Fortunately, computational experiments using more exact methods (e.g. Fuchs 1971) have shown that even in most refraction experiments the largest amplitude arrivals are generally post-critical reflections, are less often refractions, and are almost never head waves. Refractions are discussed briefly in Section 6 and will be treated in more detail elsewhere.

4.2 A MULTI-LAYERED MEDIUM

Up to this point we have assumed that the medium contains no interfaces other than Σ. Now suppose the medium has above Σ two other interfaces A and B, as shown in Fig. 6. Focusing effects associated with the curvature of interfaces A and B are automatically included in relations (13) and (14) through the factors $dA/d\Omega$ or $dl/d\theta$ in equations (15) or (16). However, to account for the loss of energy through reflections and mode changes at A and B, relations (13) and (14) must be modified by the inclusion of plane wave transmission coefficients. Equation (13) becomes

$$\mathbf{u}_1^P(\mathbf{x}) = \frac{\hat{\mathbf{t}}_1^P(\dot{P}\dot{P})_{1A}(\dot{P}\dot{P})_{1B}F_1^P \exp(i\omega T_1^P)}{\sqrt{\rho\alpha\rho_1\alpha_1}\, B_1^P} \tag{27}$$

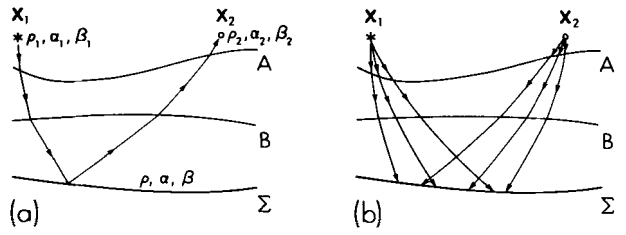

Figure 6. (a) A medium with three interfaces A, B, and Σ showing the geometrical ray for the P-wave reflected from Σ; (b) the rayfields for $\mathbf{u}_1^P$ and $\mathbf{u}_2^P$ needed to synthesize the reflection.

in which $(\dot{P}\dot{P})_{1A}$ and $(\dot{P}\dot{P})_{1B}$ are P-wave transmission coefficients through interfaces A and B, respectively, and ρ_1 and α_1 refer to the source while ρ and α refer to the point $\mathbf{x}$ on Σ^-, the upper side of Σ. Equation (14) becomes

$$\begin{aligned}\mathbf{u}_1^S(\mathbf{x}) = {} & \{\hat{\mathbf{b}}_1(\mathbf{x})\,\hat{\mathbf{b}}_1(\mathbf{x}_B^+) + \hat{\mathbf{c}}_1(\mathbf{x})\,\hat{\mathbf{c}}_1(\mathbf{x}_B^+)\} \cdot \{\hat{\mathbf{v}}_{1B}^{SS}(\dot{V}\dot{V})_{1B}\hat{\mathbf{v}}_{1B}^S + \hat{\boldsymbol{\eta}}_{1B}(\dot{H}\dot{H})_{1B}\hat{\boldsymbol{\eta}}_{1B}\} \\ & \cdot \{\hat{\mathbf{b}}_1(\mathbf{x}_B^-)\,\hat{\mathbf{b}}_1(\mathbf{x}_A^+) + \hat{\mathbf{c}}_1(\mathbf{x}_B^-)\,\hat{\mathbf{c}}_1(\mathbf{x}_A^+)\} \cdot \{\hat{\mathbf{v}}_{1A}^{SS}(\dot{V}\dot{V})_{1A}\hat{\mathbf{v}}_{1A}^S + \hat{\boldsymbol{\eta}}_{1A}(\dot{H}\dot{H})_{1A}\hat{\boldsymbol{\eta}}_{1A}\} \\ & \cdot \{\hat{\mathbf{b}}(\mathbf{x}_A^-)\,F_1^b + \hat{\mathbf{c}}(\mathbf{x}_A^-)\,F_1^c\}\frac{\exp(i\omega T_1^S)}{\sqrt{\rho\beta\rho_1\beta_1}\;B_1^S}\end{aligned} \tag{28}$$

in which $(\dot{V}\dot{V})_{1A}$ and $(\dot{H}\dot{H})_{1A}$ are, respectively, the downward SV and SH transmission coefficients through interface A with $(\dot{V}\dot{V})_{1B}$ and $(\dot{H}\dot{H})_{1B}$ playing similar roles for interface B. The vectors $\hat{\mathbf{v}}_{1A}^{SS}$, $\hat{\mathbf{v}}_{1A}^S$ and $\hat{\boldsymbol{\eta}}_{1A}$ are an obvious extension of the notation introduced in Appendix A (Fig. A1) and are all well defined in terms of $\hat{\mathbf{t}}^S(\mathbf{x}_A^-)$ and the material parameters immediately above and below interface A. The operator $\hat{\mathbf{b}}_1(\mathbf{x})\,\hat{\mathbf{b}}_1(\mathbf{x}_B^+) + \hat{\mathbf{c}}_1(\mathbf{x})\,\hat{\mathbf{c}}_1(\mathbf{x}_B^+)$, for example, takes account of the curvature and torsion of the ray in getting from the bottom of B to the top of Σ. If the material parameters change only across A, B, and Σ and are otherwise constant then these operators have no effect and may be suppressed. Equation (28) would then become

$$\begin{aligned}\mathbf{u}_1^S(\mathbf{x}) = {} & \{\hat{\mathbf{v}}_B^{SS}(\dot{V}\dot{V})_B\hat{\mathbf{v}}_B^S + \hat{\boldsymbol{\eta}}_B(\dot{H}\dot{H})_B\hat{\boldsymbol{\eta}}_B\} \cdot \{\hat{\mathbf{v}}_{1A}^{SS}(\dot{V}\dot{V})_{1A}\hat{\mathbf{v}}_{1A}^S + \hat{\boldsymbol{\eta}}_{1A}(\dot{H}\dot{H})_{1A}\hat{\boldsymbol{\eta}}_{1A}\} \\ & \cdot \{\hat{\mathbf{b}}_1(\mathbf{x}_A^-)\,F_1^b + \hat{\mathbf{c}}_1(\mathbf{x}_A^-)\,F_1^c\}\,\frac{\exp(i\omega T_1^S)}{\sqrt{\rho\beta\rho_1\beta_1}\;B_1^S}.\end{aligned} \tag{29}$$

In view of equation (27) our expression (23) for the reflected P-wave must now be modified to include a factor $(\dot{P}\dot{P})_{1A}(\dot{P}\dot{P})_{1B}(\dot{P}\dot{P})_{2A}(\dot{P}\dot{P})_{2B}$. Equations (24)–(26) must also be modified in obvious ways to include new factors like those obtained in going from (14) to (28). These modifications are straightforward but the resulting equations are very long and will be omitted. Henceforth we will assume that (23)–(26) have been modified whenever necessary to include the effects of interfaces shallower than Σ. These modifications can of course include the effects of multiple reflections and mode changes anywhere above Σ. All of the integrals (23)–(26) we have written have the form

$$\mathbf{u}(\mathbf{x}_2) = \int_{\Sigma(\mathbf{x})} \mathbf{u}_1 \cdot \mathsf{R}_{12} \cdot \mathsf{G}_2 \, d\Sigma(\mathbf{x}) \tag{30}$$

in which G_2 is the elastic Green's tensor obtained from (13) or (14) by suppressing the '$\mathbf{a}\cdot$' in F^P, F^b, F^c. Here $\mathbf{u}_1$ is the wave from the source down to Σ^- and G_2 is the wave from the

receiver down to Σ^- (since the normal to Σ points down we use Σ^- to denote the upper side of Σ and Σ^+ to denote its lower side). The interaction coefficient R_{12} in (30) is chosen to agree with the modes of $\mathbf{u}_1$ and G_2 on Σ^- without regard to the mode of these waves in the shallower portions of their respective paths. For example, with reference to Fig. 6, if $\mathbf{u}_1$ is the wave which travels from $\mathbf{x}_1$ to B as an S-wave and from B to Σ as a P-wave, and G_2 is the wave which travels from $\mathbf{x}_2$ to B as a P-wave and from B to Σ as an S-wave then R_{12} in (30) is R_{12}^{PS} given by equations (10b–g). $\mathbf{u}_1$ and G_2 may even represent waves which have been reflected one or more times from Σ before interacting, as shown in Fig. 7.

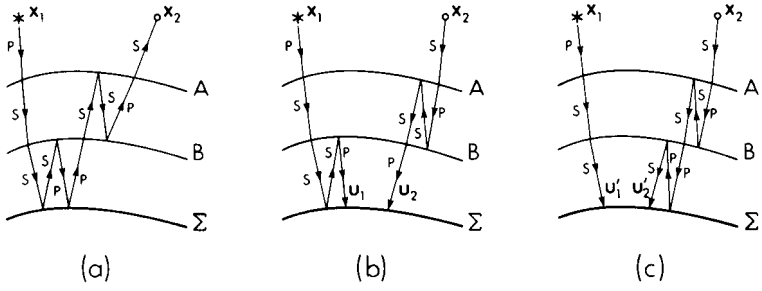

Figure 7. (a) The generalized ray whose response is to be synthesized; (b) first choice for $\mathbf{u}_1$ and $\mathbf{u}_2$; (c) a second choice for $\mathbf{u}_1$ and $\mathbf{u}_2$. Here the AB multiple has been incorporated into $\mathbf{u}'_2$ instead of $\mathbf{u}'_1$.

4.3 ATTENUATION AND DISPERSION

In an attenuating medium the Lamé parameters λ and μ become frequency dependent and complex; hence so do the seismic velocities α and β. All the quantities in the geometrical optics expressions (13) and (14) remain well defined except for travel time T and $dA/d\Omega$ (or $dl/d\theta$). To define these quantities we assume that the geometrical optics raypath is the same for all frequencies. Then $dA/d\Omega$ is frequency-independent; also, we obtain a frequency-dependent, complex travel time for the P-wave, say, by evaluating the ray path integral $T^P(\omega) = \int ds/\alpha(\omega)$ over the same path for each frequency. This definition of $T^P(\omega)$ accords with Fermat's principle, which states that, on any geometrical optics path, travel time is stationary with respect to small perturbations in the path. Thus the travel time $\int ds/\alpha(\omega)$ is nearly the same over our fixed path as it is over the true, frequency-dependent, path.

Even integrating over a frequency-independent path, evaluation of the travel times in (23)–(26) would be time consuming if many frequencies were needed. However, suppose the seismic quality factor Q is spatially homogeneous between the interfaces of the multi-layered model shown in Fig. 6. Then, even if the velocity itself is not spatially homogeneous there, we may write for the layer between, say, A and B

$$\frac{1}{\alpha(\mathbf{r},\omega)} = \frac{1}{\alpha_0(\mathbf{r})}\left[1 - \frac{1}{\pi Q_{AB}}\ln(\omega/\omega_0)\right]\exp\left(\frac{i}{2Q_{AB}}\right) \tag{31}$$

where we have assumed $\omega > 0$ and $(1/\pi Q_{AB})\ln(\omega/\omega_0) \ll 1$ (e.g. Kanamori & Anderson 1977). Here Q_{AB} and ω_0 are fixed parameters and $\alpha_0(\mathbf{r})$ is independent of frequency. Thus for the leg of the ray path between A and B

$$\int\frac{ds}{\alpha} = \left[1 - \frac{\ln(\omega/\omega_0)}{\pi Q_{AB}}\right]\exp\left(\frac{i}{2Q_{AB}}\right)\int\frac{ds}{\alpha_0}; \tag{32}$$

that is, all the frequency-dependent factors may be taken outside the integral. Doing likewise

for the other legs of the path we find that the total travel time $T_1^P(\mathbf{x})$ in equation (13) may be written

$$T_1^P(\mathbf{x}_1, \omega) = f_{1A}(\omega)\, T_{1A}^P(\mathbf{x}) + f_{AB}(\omega) T_{AB}^P(\mathbf{x}) + f_{B\Sigma}(\omega)\, T_{B\Sigma}^P(\mathbf{x}) \tag{33}$$

where f_{1A}, for example, is the coefficient of the integral on the right side of (32). Here $\mathbf{x}$ is, as usual, a point on Σ. The significance of (33) is that if we are willing to store the three functions $T_{1A}^P(\mathbf{x})$, $T_{AB}^P(\mathbf{x})$, $T_B^P(\mathbf{x})$ separately (instead of storing their sum, as we would in the lossless case) then we can quickly recover $T_1^P(\mathbf{x}, \omega)$ for each frequency. Of course, if the quality factor Q is the same in each layer then in (33) $f_{1A} = f_{AB} = f_{B\Sigma}$ and we need only save the sum of the travel times, just as in the lossless case.

4.4 LIMITATIONS OF THE METHOD

As noted above an advantage of Kirchhoff–Helmholtz (KH) theory over geometrical optics is that the former gives a correct response when the receiver is located on a caustic whereas the latter does not. However, this advantage also obtains with other methods for synthesizing reflections. The EWKBJ (Frazer & Phinney 1980) or Maslov method (Maslov 1965; Chapman & Drummond 1982) allows the receiver to be located on a caustic and so does the Gaussian beam method (e.g. Červený 1983). These two methods are probably superior to KH theory for modelling refracted waves in a medium without interfaces (Sinton & Frazer 1981; Haddon 1982, 1983). For modelling reflections, however, KH theory is probably superior to both of these other methods because of its more correct rendering of shadow arrivals and diffractions. To see why this is so consider the situation shown in Fig. 8, where a fault in a reflective interface has caused the primary reflection wavefield to divide into two branches separated by a shadow zone. Without loss of generality we may for convenience take the velocity to be unity above the reflector and take the reflector to be flat except at the fault. Travel-time curves for the synthetics that would be obtained with various methods are also shown in Fig. 8. For reference: ABE is the reflection branch that would be obtained; in the absence of a fault, from an infinite length horizontal reflector passing through P; LHJ is the reflection that would be obtained from a single infinite length horizontal reflector passing through points Q and R. The KH method gives branches ABD, CB, GHJ and HI with the arrivals on branches CB and HI opposite in polarity to arrivals on the other branches. Hilterman's (1970) experiments with physical models and sources shows that these arrivals

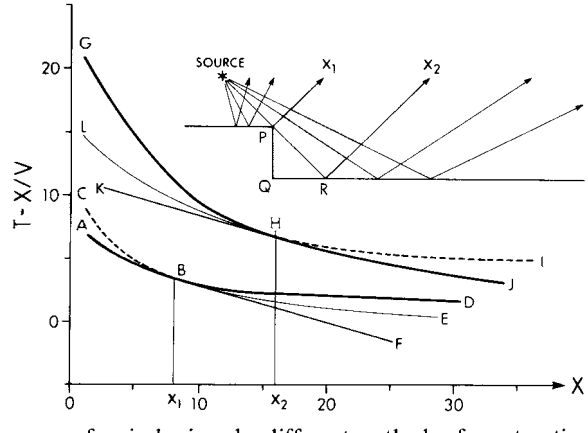

Figure 8. Travel-time curves of arrivals given by different methods of constructing synthetic seismograms for a model consisting of a faulted interface. See text for discussion.

and polarities are correct. Geometrical optics gives only branches AB and HJ and so is correct only in the limit of infinite frequency. The EWKBJ/Maslov method gives branches ABF and KHJ; BF is a straight line tangent to ABE at $\mathbf{x}_1$ and KH is a straight line tangent to LHJ at $\mathbf{x}_2$. The Gaussian beam method also gives branches ABF and KHJ. Branches BF and KH are incorrect, although for low frequencies the large beam width makes this difficult to detect (e.g. Červený 1983, figs 8 and 9). To see why the Maslov and Gaussian beam methods give spurious branches BF and KH note that branch BF is associated with the single ray (plane wave) which travels from the source to the upthrown corner of the fault P hence to $\mathbf{x}_1$, and the branch KH is associated with the ray which leaves the source at the same angle but just misses the fault corner and is reflected at R up to $\mathbf{x}_2$. Branch BF and branch KH are straight and parallel because they are associated with essentially the same plane wave. It has often been pointed out that the fundamental limitation of KH theory is that the reflecting point must be contained in an area of surface whose linear dimensions and radii of curvature are large compared to a wavelength. The example of Fig. 8 indicates that the key word in this statement is 'contained' since KH theory works well when the reflecting point is on the boundary of such an area but the other ray methods (geometrical optics, Maslov, Gaussian beams) work only when the reflecting point is near the centre of such an area.

In any comparison of asymptotic methods correctness is, of course, a relative term. For instance, a very careful comparison of data with KH synthetics for arrivals on branches CB and HI in Fig. 8 would reveal a lack of agreement in the phase shift at low frequencies due to the fact that the region of the fault from Q to R is not truly shadowed but instead is lit by energy diffracted from the corner P. Also, depending on the nature of the velocity jump across the interface in Fig. 8, we would expect to see a head wave arrival from either the upthrown side of the interface or the downthrown side. The KH theory presented here will not give this arrival because it assumes only a single interaction with the interface. This lack of head waves will be particularly serious in a situation like that shown in Fig. 9 where the upthrown side of the interface is rounded off. If velocity increases across the interface then the incident field will excite a rather strong whispering gallery wave which will radiate upwards; but this wave will be absent from our KH synthetics. Stephen (1984) has observed such a wave in marine data and modelled it using a finite difference method. Such waves could also be modelled using the boundary integral equation method (e.g. Cole, Kosloff & Minster 1978).

The most significant limitation of the KH theory outlined above is one to which the Maslov and Gaussian beam methods are not subject. It is encountered when the wavefields $\mathbf{u}_1$ and $\mathbf{u}_2$ in the integral (3) cannot be represented everywhere on Σ by the geometrical optics equations (13) and (14). Consider the situation shown in Fig. 10. There the velocity structure is such that the $\mathbf{u}_1^P$ rayfield (from the source) has two caustics on Σ. The geometrical optics representation of $\mathbf{u}_1^P$ on Σ is a sum of three terms of the form (13). At each of the caustics on Σ, two of the three terms will be singular due to a zero of their

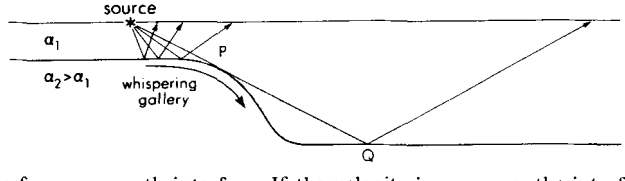

Figure 9. Reflections from a smooth interface. If the velocity jump across the interface is positive then a whispering gallery wave will be excited in the upper portion of the curved part of the interface and will propagate past *P* into the shadow, radiating upward. This energy will be absent from our KH reflection synthetics.

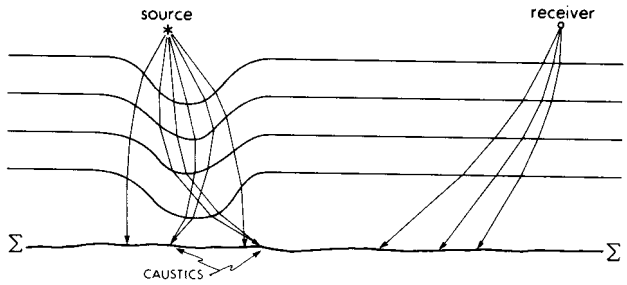

Figure 10. The problem with the KH method when the medium is inhomogeneous above the reflector of interest is that $\mathbf{u}_1$ or $\mathbf{u}_2$ may have caustics on Σ. Then the geometrical optics expressions for $\mathbf{u}_1$ and $\mathbf{u}_2$ are no longer valid.

spreading factors. When the representation for $\mathbf{u}_1^P$ is substituted into (22a) the resulting integrand is therefore a sum of three terms each of which has a different phase function and each of which is singular at one or two points on Σ. It can be seen that in general, if $\mathbf{u}_1$, the wave from the source to Σ, is a sum of m terms of the form (13) and $\mathbf{u}_2$, the wave from the receiver to Σ, is a sum of n terms of the form (13) then the resulting integrand of (22a) is a sum of mn terms each of which has a different phase function and is singular at one or two points on Σ. Let us denote such a term by $\mathbf{f}_k \exp(i\phi_k)$, $1 < k < mn$; then $\phi_k = \omega(T^P_{1i} + T^P_{2j})$ for some i and j in the ranges $1 < i < m$ and $1 < j < n$, respectively. Each reflection arrival from Σ is associated with a stationary point of some function ϕ_k. Thus if no ϕ_k is stationary near the singularities of its $\mathbf{f}_k$ we can compute all of our arrivals by limiting the range of integration to exclude the singularities. However, limiting the range of integration is unsatisfactory in several respects: it requires determining the location of stationary points before integrating; it gives synthetics with unreliable amplitudes, or truncation phases; and there is no guarantee that a stationary point of some ϕ_k will not coincide with a singularity of $\mathbf{f}_k$.

Another approach to this problem was taken by Sinton & Frazer (1981), who treated the singularities of each $\mathbf{f}_k$ as integrable and integrated over them. This procedure makes it unnecessary to locate the stationary points of the ϕ_k before integrating; however, it too is unsatisfactory in several respects: the integrable singularities cause small spurious arrivals; if a stationary point of ϕ_k coincides with a singularity of $\mathbf{f}_k$ then the amplitude of the arrival associated with that stationary point is unreliable; and, finally, not all the singularities of geometrical optics formulae are integrable. In a variation on this approach Sen & Frazer (1983) proposed that the integrable singularities could be removed from each term $\mathbf{f}_k \exp(i\phi_k)$ by convolving each $\mathbf{f}_k(\mathbf{x})$ with a smoothing operator whose width is a decreasing function of frequency. This enlarges the domain of $\mathbf{f}_k(\mathbf{x})$ and so the phase function $\phi_k(\mathbf{x})$ must be extrapolated to cover this enlarged domain. This procedure has a number of advantages: the spurious phases associated with the singularities are no longer present; the integrand is still a sum of terms $\mathbf{f}_k \exp(i\phi_k)$ each of which has a well-defined phase function ϕ_k; we know that physically the singularities do not exist at finite frequencies, therefore any method of quelling them is better than not quelling them at all; on the other hand it seems clear that if we are to average $\mathbf{f}_k$ in order to quell its singularities we ought to average it over a wavefront instead of a surface on which ϕ_k also varies. If we averaged over a wavefront our frequency-dependent smoothing operator would then play a role similar to the beam amplitude profile in the Gaussian beam theory. Deregowski & Brown (1983) have used such a scheme in numerical calculations; they average over the surface containing the receivers instead of a wavefront, and do not bother to extend the domain of $\phi_k(\mathbf{x})$. In

summary, although the physical basis of such a procedure may be reasonable its mathematics have not yet been worked out and may in fact not be workable since, as noted above, a geometrical optics formula may well have a non-integrable singularity. In the next section we consider in detail a quite different approach to the problem of caustics on Σ.

5 One-fold path integrals

Earlier we noted that the KH integral for the generalized ray shown in Fig. 7(a) could be written in two ways. In the first way we write

$$\hat{\mathbf{a}}_2 \cdot \mathbf{u}_1(\mathbf{x}_2) = \int_\Sigma \mathbf{u}_1 \cdot \mathsf{R}_{12}^{PP} \cdot \mathbf{u}_2 \, d\Sigma \tag{34}$$

using the interaction coefficient given by (9b) and the geometrical optics expressions for $\mathbf{u}_1$ and $\mathbf{u}_2$ shown in Fig. 7(b). In the second way we write

$$\hat{\mathbf{a}}_2 \cdot \mathbf{u}_1(\mathbf{x}_2) = \int_\Sigma \mathbf{u}_1' \cdot \mathsf{R}_{12}^{SS} \cdot \mathbf{u}_2' \, d\Sigma \tag{35}$$

using the interaction coefficient given by (12b) and the geometrical optics expressions for $\mathbf{u}_1$ and $\mathbf{u}_2$ shown in Fig. 7(c). If none of the rayfields in Fig. 7 has a caustic on Σ then (34) and (35) are equivalent. However, it may happen that $\mathbf{u}_1$ or $\mathbf{u}_2$ has a caustic on Σ whereas $\mathbf{u}_1'$ and $\mathbf{u}_2'$ do not. Then equation (35) will have an integrand consisting of a single term of the form $\mathbf{f}\exp(i\omega\phi)$ where $\mathbf{f}$ is regular, whereas equation (34) will have an integrand of the form $\Sigma_k \mathbf{f}_k \exp(i\phi_k)$ where each $\mathbf{f}_k$ is singular. That is, equation (35) will be accurate and easy to evaluate by the method of this paper but equation (34) will be plagued by all the difficulties described in Section 4.4. Frazer (1983) showed that (34) and (35) are both one-fold path integrals that can be derived from the same nine-fold path integral by different applications of the method of stationary phase. [Frazer (1983) referred to these path integrals as Feynman path integrals (Feynman & Hibbs 1964), but this is incorrect. An actual application of the Feynman technique to the wave equation is given by Schulman (1981, p. 164).] Details of the theory of multi-fold integrals for reflection problems will be the subject of a separate paper but we summarize the theory here in order to exhibit the relation between (34) and (35) and to show how to find other one-fold integrals for the same generalized ray.

For simplicity consider once more the *P*-wave shown in Fig. 6(a). The path shown in Fig. 6(a) is a geometrical optics path; actually the energy in the *P*-wave reflected from Σ may be regarded as travelling from the source to every point on A, from every point on A to every point on B, from every point on B to every point on Σ then from every point on Σ upward to every point on B, from every point on B to every point on A and from every point on A to the receiver. Paths such as the one shown in Fig. 11(a) are thus legitimate. The integral giving the contribution of all such paths may be written

$$\hat{\mathbf{a}}_2 \cdot \mathbf{u}_1(\mathbf{x}_2) = \int_A dA \int_B dB \int_\Sigma d\Sigma \int_B dB' \int_A dA' \frac{f(\mathbf{x}_1, \mathbf{x}_A, \mathbf{x}_B, \mathbf{x}_\Sigma, \mathbf{x}_B', \mathbf{x}_A', \mathbf{x}_2)}{R_{1A}R_{AB}R_{B\Sigma}R_{\Sigma B}R_{BA}R_{A2}}$$
$$\times \exp\left\{i\omega\left(\frac{R_{1A}}{\alpha_A} + \frac{R_{AB}}{\alpha_B} + \frac{R_{B\Sigma}}{\alpha_\Sigma} + \frac{R_{\Sigma B}}{\alpha_\Sigma} + \frac{R_{BA}}{\alpha_B} + \frac{R_{A2}}{\alpha_A}\right)\right\} \tag{36}$$

where for brevity we have taken the velocity to be constant between interfaces. In this expression $R_{1A} = \| \mathbf{x}_1 - \mathbf{x}_A \|$, $R_{AB} = \| \mathbf{x}_A - \mathbf{x}_B \|$, $R_{B\Sigma} = \| \mathbf{x}_B - \mathbf{x}_\Sigma \|$, $R_{\Sigma B} = \| \mathbf{x}_\Sigma -$

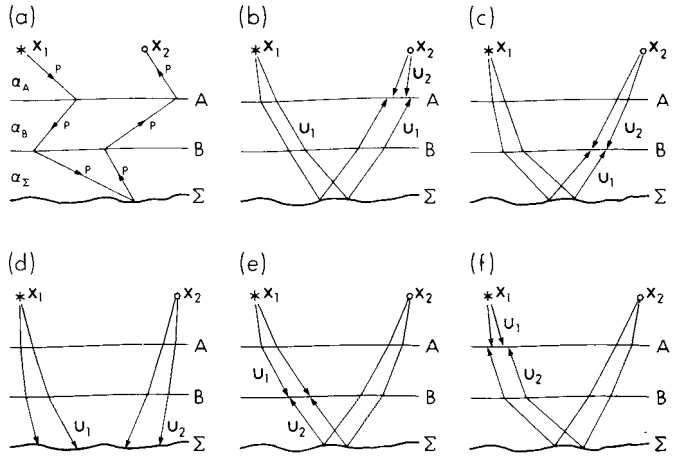

Figure 11. (a) One of the paths summed in the five-fold path integral (36) for the *P*-wave of Fig. 6(a); (b) the one-fold integral that would be obtained if the first four integrals in (36) were evaluated simultaneously by the method of stationary phase. Similarly for: (c) the first, second, third and fifth integrals; (d) the first, second, fourth and fifth integrals; (e) the first, third, fourth and fifth integrals; (f) the second, third, fourth and fifth integrals.

$\mathbf{x}'_B \|$, $R_{BA} = \| \mathbf{x}'_B - \mathbf{x}'_A \|$, $R_{A2} = \| \mathbf{x}'_A - \mathbf{x}_2 \|$, dA is the element of area on interface A and similarly for the other interfaces, and $f(\mathbf{x}_1, \mathbf{x}_A, \mathbf{x}_B, \mathbf{x}_\Sigma, \mathbf{x}'_B, \mathbf{x}'_A, \mathbf{x}_2)$ is a product of interaction coefficients similar to those used in this paper. If we were to apply the method of stationary phase to (simultaneously) the first, second, fourth and fifth integrals in (36) we would obtain exactly the KH integral (34) with $\mathbf{u}_1$ and $\mathbf{u}_2$ given by the geometrical optics expression for the rays in Fig. 11(d). This is the kind of integral we have been treating in this paper. On the other hand if we were to apply the method of stationary phase to (simultaneously) the first four integrals in (36) we would obtain an integral like (34) – the interaction coefficient will be slightly different – with $\mathbf{u}_1$ and $\mathbf{u}_2$ given by the geometrical optics expressions for the rays in Fig. 11(b).

Fortunately we do not actually have to write out the exact form of (36) and perform the stationary phase evaluation of four integrals to get whichever one-fold integral we seek. We can use the KH formalism to obtain the one-fold integral directly. For example, to obtain the one-fold integral which uses the $\mathbf{u}_1$ and $\mathbf{u}_2$ shown in Fig. 11(c) note first that since $\mathbf{u}_1$ has been reflected upward from Σ it appears to emanate from a virtual source distribution *below* interface B. As shown in Fig. 12 we may apply the KH equation (5) with $B \subset \partial V$ and $\hat{\mathbf{n}} = \hat{\mathbf{n}}_B$. By an analysis very similar to that given in Section 2 we obtain

$$\hat{\mathbf{n}} \cdot (\boldsymbol{\tau}_1^P \cdot \mathbf{u}_2^{PP} - \boldsymbol{\tau}_2^{PP} \cdot \mathbf{u}_1^P) = \mathbf{u}_1^P \cdot \mathbf{D}_{12}^{PP} \cdot \mathbf{u}_2^P \tag{37a}$$

in which

$$\mathbf{D}_{12}^{PP} = \{\lambda(\hat{\mathbf{t}}_1^P \hat{\mathbf{n}} - \hat{\mathbf{n}} \hat{\mathbf{t}}_2^{PP}) + 2\mu(\hat{\mathbf{n}} \hat{\mathbf{t}}_1^P - \hat{\mathbf{t}}_2^{PP} \hat{\mathbf{n}}\} \cdot \hat{\mathbf{t}}_2^{PP} \frac{i\omega}{\alpha} (\dot{P}\dot{P})_2 \hat{\mathbf{t}}_2^P. \tag{37b}$$

To make each term in (37b) well-defined we denote the $-\hat{\mathbf{n}}_B$ (upper) side of surface B by B^- and the $+\hat{\mathbf{n}}_B$ (lower) side of B by B^+. Since λ, μ and α are discontinuous across B we denote values of λ on the upper side of B by $\lambda(\mathbf{x}_B^-)$ and values of λ on the lower side of B by $\lambda(\mathbf{x}_B^+)$ and similarly for μ and α. In (37b) $\lambda = \lambda(\mathbf{x}_B^+)$, $\mu = \mu(\mathbf{x}_B^+)$, $\alpha = \alpha(\mathbf{x}_B^+)$, $(\dot{P}\dot{P})_2$ is for

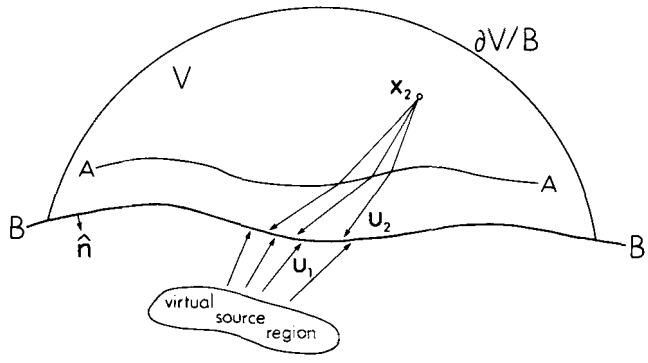

Figure 12. Using KH theory to calculate the one-fold integral for Fig. 11(c). We take $B \subset \partial V$ and note that $\mathbf{u}_1$ appears to emanate from outside V. As usual the integration over $\partial V \backslash B$ is neglected.

a P-wave incident from above B with direction of propagation $\hat{\mathbf{t}}_2^P$ (see Appendix A), and

$$\hat{\mathbf{t}}_2^{PP} = \alpha(\mathbf{x}_B^+)\,\sigma\hat{\boldsymbol{\sigma}} + \sqrt{1-\alpha(\mathbf{x}_B^+)^2\sigma^2}\,\hat{\mathbf{n}}; \tag{37c}$$

$$\boldsymbol{\sigma} = \mathbf{t}_2^P \cdot (\mathbf{I} - \mathbf{nn})/\alpha(\mathbf{x}_B^-),\ \sigma = ||\,\boldsymbol{\sigma}\,||,\ \hat{\boldsymbol{\sigma}} = \boldsymbol{\sigma}/\sigma. \tag{37d}$$

Then

$$\hat{\mathbf{a}}_2 \cdot \mathbf{u}_1(\mathbf{x}_2) = \int_B \mathbf{u}_1^P \cdot \mathbf{D}_{12}^{PP} \cdot \mathbf{u}_2^P\, dB \tag{37e}$$

is the one-fold integral for Fig. 11(c).

It is interesting to compare (37b) with equation (9b). In deriving (37b) we used a plane wave transmission coefficient to transmit $\mathbf{u}_2$ downward through surface B, then used the PP interaction equation (8); in deriving (9b) we used a plane wave reflection coefficient to reflect $\mathbf{u}_1$ upward from Σ and then used equation (8). We could have obtained a different looking expression for (9b) by reflecting $\mathbf{u}_2$ instead of $\mathbf{u}_1$ and we can obtain an alternative expression for (37b) by transmitting $\mathbf{u}_1$ instead of $\mathbf{u}_2$. Doing so yields

$$\hat{\mathbf{n}} \cdot (\boldsymbol{\tau}_1^{PP} \cdot \mathbf{u}_2^P - \boldsymbol{\tau}_2^P \cdot \mathbf{u}_1^{PP}) = \mathbf{u}_1^P \cdot \mathbf{E}_{12}^{PP} \cdot \mathbf{u}_2^P \tag{38a}$$

in which

$$\mathbf{E}_{12}^{PP} = \hat{\mathbf{t}}_1^P(\acute{P}\acute{P})_1 \frac{i\omega}{\alpha}\hat{\mathbf{t}}_1^{PP} \cdot \{\lambda(\hat{\mathbf{t}}_1^{PP}\hat{\mathbf{n}} - \hat{\mathbf{n}}\hat{\mathbf{t}}_2^P) + 2\mu(\hat{\mathbf{n}}\hat{\mathbf{t}}_1^{PP} - \hat{\mathbf{t}}_2^P\hat{\mathbf{n}})\} \tag{38b}$$

where $\lambda = \lambda(\mathbf{x}_B^-)$, $\mu = \mu(\mathbf{x}_B^-)$, $\alpha = \alpha(\mathbf{x}_B^-)$, $(\acute{P}\acute{P})_2$ is for a P-wave incident from below B with direction of propagation $\hat{\mathbf{t}}_1^P$, and

$$\hat{\mathbf{t}}_1^{PP} = \alpha(\mathbf{x}_B^-)\,\sigma\hat{\boldsymbol{\sigma}} - \sqrt{1-\alpha(\mathbf{x}_B^-)^2\sigma^2}\,\hat{\mathbf{n}} \tag{38c}$$

$$\boldsymbol{\sigma} = \mathbf{t}_1^P \cdot (\mathbf{I} - \mathbf{nn})/\alpha(\mathbf{x}_B^+),\ \sigma = ||\,\sigma\,||,\ \hat{\boldsymbol{\sigma}} = \boldsymbol{\sigma}/\sigma. \tag{38d}$$

Then

$$\hat{\mathbf{a}}_2 \cdot \mathbf{u}_1(\mathbf{x}_2) = \int_B \mathbf{u}_1^P \cdot \mathbf{E}_{12}^{PP} \cdot \mathbf{u}_2^P\, dB \tag{38e}$$

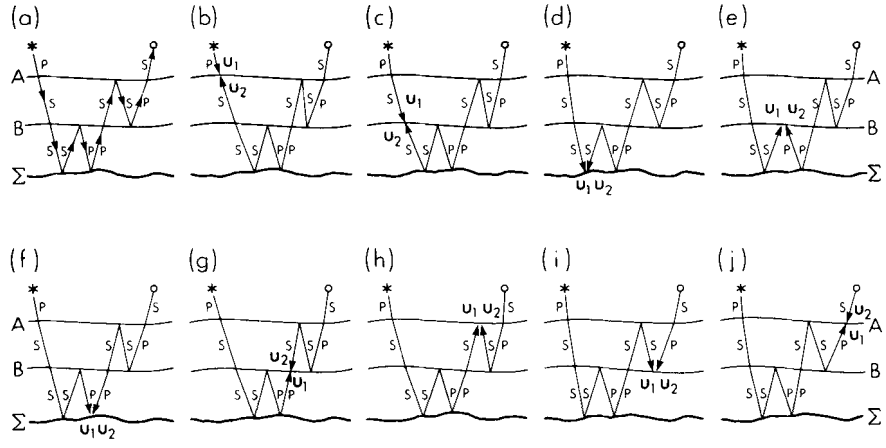

Figure 13. The generalized ray in (a) may be written as a nine-fold path integral (equation 39) or a one-fold integral (KH integral) using any one of the geometrical optics ray pairs in (b)–(j).

is also the one-fold integral for Fig. 11(c). Although (37b) and (38b) look quite different they take the same values on neighbourhoods of stationary points of (37e) and (38e). Thus they are identical within the accuracy of the rest of our theory. The other interaction coefficients for transmission, D_{12}^{PS}, D_{12}^{SP}, D_{12}^{SS} (or equivalently E_{12}^{PS}, E_{12}^{SP}, E_{12}^{SS}) are straightforward to obtain using equation (8) and (9) and will be omitted.

We return briefly to the more complicated generalized ray of Fig. 7(a), repeated in Fig. 13(a). The full-fold path integral for this ray is

$$\begin{aligned}\mathbf{a}_2\mathbf{u}_1(\mathbf{x}_2) = & \int_A dA \int_B dB \int_\Sigma d\Sigma \int_B dB' \int_\Sigma d\Sigma' \int_B dB'' \int_A dA' \int_B dB''' \int_A dA'' \\ & \times f(\mathbf{x}_1, \mathbf{x}_A, \mathbf{x}_B, \mathbf{x}_\Sigma, \mathbf{x}'_B, \mathbf{x}'_\Sigma, \mathbf{x}''_B, \mathbf{x}'_A, \mathbf{x}'''_B, \mathbf{x}''_A, \mathbf{x}_2) \\ & \times \exp\left\{i\omega\left(\frac{R_{1A}}{\alpha_A}+\frac{R_{AB}}{\beta_B}+\frac{R_{B\Sigma}}{\beta_\Sigma}+\frac{R_{\Sigma B'}}{\beta_\Sigma}+\frac{R_{B'\Sigma'}}{\alpha_\Sigma}+\frac{R_{\Sigma' B''}}{\alpha_\Sigma}+\frac{R_{B''A'}}{\beta_B}+\frac{R_{A'B'''}}{\beta_B}\right.\right. \\ & \left.\left.+\frac{R_{B'''A''}}{\alpha_B}+\frac{R_{A''2}}{\beta_A}\right)\right\} \\ & \times (R_{1A}R_{AB}R_{B\Sigma}R_{\Sigma B'}R_{B'\Sigma'}R_{\Sigma' B''}R_{B''A'}R_{A'B'''}R_{B'''A''}R_{A''2})^{-1} \qquad (39)\end{aligned}$$

where again for brevity we have assumed that density and velocities are constant between interfaces. In this expression $R_{1A} = \| \mathbf{x}_1 - \mathbf{x}_A \|$, $R_{AB} = \| \mathbf{x}_A - \mathbf{x}_B \|$, and so forth, and f is a product of interaction coefficients. Full fold integrals such as (39) and (36) are always robust with respect to internal caustics but they are time-consuming to compute (clearly!) and are usually not needed. If for one of the geometrical optics pairs $(\mathbf{u}_1, \mathbf{u}_2)$ in Fig. 13(b–j) neither $\mathbf{u}_1$ nor $\mathbf{u}_2$ has a caustic, then the KH integral which uses that pair will be just as robust. In order to determine whether such a pair exists it is only necessary to trace two sets of rays. For the problem in Fig. 13 one set of geometrical optics rays, the $\mathbf{u}_1$-set, say, is traced from the source along paths similar to $\mathbf{u}_1$ in Fig. 13(j). Another set of geometrical optics rays, the $\mathbf{u}_2$-set, is traced from the receiver along paths similar to $\mathbf{u}_2$ in Fig. 13(b). If for one of the (virtual) interface $C \in \{A, B, \Sigma, B', \Sigma', B'', A', B''', A''\}$ the $\mathbf{u}_1$-set has no caustics on or before C and the $\mathbf{u}_2$ set has no caustics on or before C then C is a good

surface of integration for a KH integral. Of course if no good surface C exists then we can consider going to a two-fold path integral. We do not discuss two-fold path integrals here except to note that for the generalized ray of Fig. 13(a) there are $\binom{9}{2} = 36$ possible two-fold integrals, and a great many sets of rays must be traced to verify visually the goodness of even one of them. Note, however, that in Fig. 13 we have not exhausted the possibilities for one-fold integrals since we are free to choose a surface of integration across which velocity does not change. With reference to Fig. 13 suppose: C and C' are adjacent virtual surfaces; that $\mathbf{u}_1$ has caustics on C' but not C, and that $\mathbf{u}_2$ has caustics on C but not C'. Then there may be a good surface of integration between C and C'. Also, every one-fold integral is implicitly an integration over the focal spheres of the source and receiver. Thus we are free to allocate different portions of the focal sphere to different one-fold integrals and then sum these integrals to get the complete response. Since the $\mathbf{u}_1$- and $\mathbf{u}_2$-ray sets introduced above give the correspondence between the reflector surface and the focal spheres, inspection of these ray sets will indicate which portions of the focal spheres should be allocated to which one-fold integrals.

6 Refracted waves

As a simple example we consider the situation shown in Fig. 14. We take the material parameters to be linear both above and below the surface Σ but discontinuous across Σ.

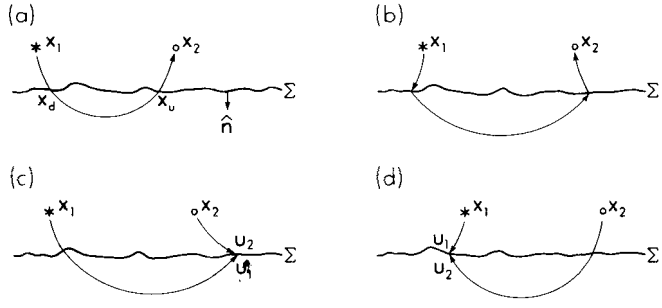

Figure 14. Single interface problem for a refracted wave. In this model the material parameters are (different) linear functions of position above and below Σ; (a) the geometrical optics path between $\mathbf{x}_1$ and $\mathbf{x}_2$; (b) an admissible path in the full (two)-fold path integral; (c) and (d) possible one-fold path integrals for the phase in (a).

Thus for P-wave velocity: above Σ, $\alpha(\mathbf{r}) = \alpha(\mathbf{r} - \mathbf{r}_a) \cdot \mathbf{w}_a$ and below Σ, $\alpha(\mathbf{r}) = (\mathbf{r} - \mathbf{r}_b) \cdot \mathbf{w}_b$ for some constant vectors $\mathbf{r}_a$, $\mathbf{w}_a$, $\mathbf{r}_b$ and $\mathbf{w}_b$. Fig. 14(a) shows a geometrical optics path between $\mathbf{x}_1$ and $\mathbf{x}_2$. To synthesize the P-wave associated with this path we may use the full-fold path integral

$$\hat{\mathbf{a}}_2 \cdot \mathbf{u}_1(\mathbf{x}_2) = \int_\Sigma d\Sigma \int_\Sigma d\Sigma' \, f(\mathbf{x}_1, \mathbf{x}_\Sigma, \mathbf{x}'_\Sigma, \mathbf{x}_2) \frac{\exp\{i\omega(T_{1\Sigma} + T_{\Sigma\Sigma'} + T_{\Sigma'2})\}}{B_{1\Sigma} B_{\Sigma\Sigma'} B_{\Sigma'2}} \tag{40}$$

in which $T_{1\Sigma}$, $T_{\Sigma\Sigma'}$, $T_{\Sigma'2}$ are the travel times from $\mathbf{x}_1$ to $\mathbf{x}_\Sigma$, $\mathbf{x}_\Sigma$ to $\mathbf{x}'_\Sigma$, and $\mathbf{x}'_\Sigma$ to $\mathbf{x}_2$, respectively: $B_{1\Sigma}$, $B_{\Sigma\Sigma'}$, $B_{\Sigma'2}$ are spreading factors; and $\mathbf{f}(\mathbf{x}_1, \mathbf{x}_\Sigma, \mathbf{x}'_\Sigma, \mathbf{x}_2)$ is a product of interaction coefficients. [At a stationary phase point of (40) f will be proportional to $\dot{P}\dot{P}(\mathbf{x}_d)\,\dot{P}\dot{P}(\mathbf{x}_u)$ where $\mathbf{x}_u$ and $\mathbf{x}_d$ are the upward and downward points, respectively, of the

geometrical ray in Fig. 14(a).] Application of the method of stationary phase to the integration over Σ' in equation (40) yields the one-fold path integral (Kirchhoff–Helmholtz integral)

$$\hat{\mathbf{a}}_2 \cdot \mathbf{u}_1(\mathbf{x}_1) = \int d\Sigma\, \mathbf{u}_1 \cdot \mathsf{E}_{12}^{PP} \cdot \mathbf{u}_2 \tag{41}$$

where $\mathbf{u}_1$ and $\mathbf{u}_2$ are shown in Fig. 14(c) and E_{12}^{PP} is given by (38b). On the other hand, application of the method of stationary phase to the integration over Σ in (40) yields the one-fold integral

$$\hat{\mathbf{a}}_2 \cdot \mathbf{u}_1(\mathbf{x}_2) = \int_{\Sigma} d\Sigma' \mathbf{u}_2 \cdot \mathsf{E}_{12}^{PP} \cdot \mathbf{u}_1 \tag{42}$$

where $\mathbf{u}_1$ and $\mathbf{u}_2$ are shown in Fig. 14(d). To see whether (41) or (42) is robust (i.e. whether neither $\mathbf{u}_1$ nor $\mathbf{u}_2$ has caustics on Σ) we trace one set of rays from the source, down through Σ, through their turning points and back up to Σ; and a similar set of rays from the receiver, down through Σ, through their turning points and back up to Σ.

Integrals (40)–(42) are for waves that interact only twice with Σ, but a similar procedure can be used for refracted waves that reflect off the bottom of the interface. For example, a wave with three turning points in the lower medium will give rise to a four-fold integral analogous to (40) and four equivalent one-fold integrals. The tracing of one set of rays from the receiver and one set of rays from the source will reveal whether any of these one-fold integrals are robust. It is clear that the total interaction of the incident field with the interface can be written formally as an infinite series of multi-fold integrals (one for each generalized ray), of which integral (40) is a single term. However, numerical evaluation of this series would certainly be a very inefficient way of computing the total response.

7 Discussion

In this paper we have attempted to show how Kirchhoff–Helmholtz (KH) theory can be extended to elastic media, especially multi-layered elastic media. Throughout we have assumed that the frequencies in the signal that is to be synthesized are sufficiently high that, were it not for the presence of caustics and diffractions, our methods could be replaced by geometrical optics. Thus all of our results are asymptotic. However, the experience of many workers over the past two decades in modelling body wave amplitudes and arrival times with geometrical optics suggests that such asymptotic theories are useful. Also, comparison of such theories with both experiments (e.g. Hilterman 1970) and more accurate methods (e.g. Choy *et al.* 1980) reveals that they generally work well at frequencies far lower than the mathematics would lead one to expect.

The extension of KH theory to the case of a single interface between two *elastic* media, carried out in Section 4.1, is relatively straightforward, consisting mainly in the inclusion of an elastic reflection coefficient and the use of the more general KH formula given by equation (5). The main limitation of this extension is that the reflected wave is assumed to have interacted only once with the boundary, so that head waves, for example, are not included. Section 6 shows that waves which interact numerous times with the interface can be computed using KH theory but that additional KH integrals are required to compute them. The contributions of these other waves cannot be included in the KH integral for the primary reflection. Another limitation of the extension arises in consequence of our use of a

plane wave reflection coefficient. Computational experiments in Sen & Frazer (in preparation) show that rapid changes in the reflection coefficient with angle of incidence can give rise to small erroneous arrivals in the KH synthetic seismogram.

The extention of KH theory to a multi-layered medium, in Section 4.2, is accomplished by including plane wave transmission coefficients for intermediate interfaces. With reference to Fig. 6, note that even though the energy flow is from $\mathbf{x}_1$, down to Σ, then up to $\mathbf{x}_2$, we use *downward* transmission coefficients for both the downward and upward paths through interfaces A and B. (The reason is that for reasons of convenience we calculate the spreading factor B_2^P on Σ by tracing rays from the receiver to Σ. If we were to use *upward* transmission coefficients for the upward leg then to be correct we would have to calculate B_2^P by shooting rays upward from each point of Σ to a neighbourhood of the receiver.) The procedure given in Section 4.2 works well even if the receiver is located on a caustic but breaks down if either the source wavefield or the receiver wavefield has a caustic on the reflector Σ, for Σ is the surface of integration. The nature of the breakdown is discussed in Section 4.4. Numerical examples will be given in Sen & Frazer (in preparation), and have already been given for a similar situation by Frazer & Sinton (1984).

The breakdown in the method of Section 4.2 can often be avoided by using a surface of integration other than the reflector. As shown in Section 5 all such one-fold integrals are derivable from a multifold path integral. For a medium consisting of homogeneous irregular layers the most general path integral that might be required to synthesize a primary reflection is the one with a single integration over the reflector and two integrations over each intermediate interface; we refer to this integral as the full-fold path integral. With the full-fold integral we associate a generalized ray or path like the one shown in Fig. 11(a). This generalized ray obeys Snell's law between interfaces but is non-Snell at each interface. If one of the integrations in the full-fold integral is evaluated by stationary phase then the result is a lower-fold integral whose associated generalized ray now has a Snell-type interaction at one interface. Continuing this procedure leaves a one-fold integral whose generalized ray has a Snell-type interaction with every interface but one. Seen from this point of view, the KH integral over the reflector is just one member of a family of one-fold integrals. Fortunately, as shown in Section 5, all of these one-fold integals can be derived directly with the KH theory of Section 4.2; it is not necessary actually to perform stationary phase on a full-fold integral. Frazer (1983) showed an example of the breakdown of the KH integral and calculated the reflection using a one-fold integral over an intermediate interface. Other examples will be given in Sen & Frazer (in preparation).

Unfortunately there are many velocity models that will give reflections for which no member of the family of one-fold integrals is robust. In such situations a multifold integral must be used. A detailed derivation of the full-fold path integral, including generalized transmission coefficients, will be given elsewhere. It is interesting to note that similar path integrals have already been used for the synthesis of refracted waves in a smoothly varying acoustic medium by Haddon (1983) and Zherniak (1983). Haddon (private communication) has stated that the amount of ray tracing required makes this method prohibitively expensive. However, in the refraction problem treated by Haddon (1983), velocity could not be held constant between surfaces of integration and rays had to be traced numerically from surface to surface. For the reflection problem, one can choose models with velocity constant between surfaces of integration so that ray paths are piecewise straight and easily calculated.

Acknowledgments

We thank S. Mallick, D. A. Lindwall, M. M. Rowe and J. F. McMillan for helpful discussions

and John J. McCoy for pointing out that the multifold integrals referred to in this paper are not Feynman path integrals. Paul Fowler drew our attention to Zherniak's work and Chuck Sword provided a translation. This research was supported by the US Office of Naval Research. Hawaii Institute of Geophysics Contribution No. 1549.

References

Aki, K. & Richards, P. G., 1980. *Quantitative Seismology: theory and methods*, volume 1, W. H. Freeman & Co., San Francisco.

Babich, V. M. & Alekseev, A. S., 1958. The ray method for calculating the intensity of wavefronts, *Bull. Acad. Sci. USSR, Geophys. Ser.*, **1**, 9–15.

Backus, G. E., 1967. Converting vector and tensor equations to scalar equations in spherical coordinates, *Geophys. J. R. astr. Soc.*, **13**, 41–101.

Berryhill, J. R., 1977. Diffraction response for nonzero separation of source and receiver, *Geophysics*, **42**, 1158–1176.

Berryhill, J. R., 1979. Wave-equation datuming, *Geophysics*, **44**, 1329–1344.

Burridge, R., 1962. The reflection of high-frequency sound in a liquid sphere, *Proc. R. Soc. A*, **270**, 144–154.

Burridge, R., 1963. The reflection of a pulse in a solid sphere, *Proc. R. Soc. A*, **276**, 367–400.

Burridge, R. & Knopoff, L., 1964. Body force equivalents for seismic dislocations, *Bull. seism. Soc. Am.*, **54**, 1875–1888.

Carter, J. A. & Frazer, L. N., 1983. A method for modelling reflection data from media with lateral velocity changes, *J. geophys. Res.*, **88**, 6469–6476.

Červený, V., 1983. Synthetic body wave seismograms for laterally varying layered structures by the Gaussian beam method, *Geophys. J. R. astr. Soc.*, **73**, 389–426.

Červený, V. & Hron, F., 1980. The ray series method and dynamic ray tracing system for three-dimensional inhomogeneous media, *Bull. seism. Soc. Am.*, **70**, 47–77.

Červený, V., Mołotkov, I. A. & Pšenčík, 1977. *Ray Method in Seismology*, Univerzita Karlova Praha.

Chapman, C. H. & Drummond, R., 1982. Body-wave seismograms in inhomogeneous media using Maslov asymptotic theory, *Bull. seism. Soc. Am.*, **72**, S277–S317.

Choy, G. L., Cormier, V. F., Kind, R., Muller, G. & Richards, P. G., 1980. A comparison of core phases generated by the full wave theory and by the reflectivity method, *Geophys. J. R. astr. Soc.*, **61**, 21–39.

Cole, D. M., Kosloff, D. D. & Minster, J. B., 1978. A numerical boundary integral equation method for elastodynamics. I, *Bull. seism. Soc. Am.*, **68**, 1331–1357.

de Hoop, A. T., 1958. Representation theorems for the displacement in an elastic solid and their application to elastodynamic diffraction theory, *Doctoral dissertation*, Technische Hogeschool, Delft.

Deregowski, S. M. & Brown, S. M., 1983. A theory of acoustic diffractors applied to 2-D models, *Geophys. Prospect.*, **31**, 293–333.

Feynman, R. P. & Hibbs, A. R., 1964. *Quantum Mechanics and Path Integrals*, McGraw-Hill, New York.

Frazer, L. N., 1983. Feynman path integral synthetic seismograms, *Eos, Trans. Am. geophys. Un.*, **64**, 772.

Frazer, L. N. & Phinney, R. A., 1980. The theory of finite frequency synthetic seismograms in inhomogeneous elastic media, *Geophys. J. R. astr. Soc.*, **63**, 691–717.

Frazer, L. N. & Sinton, J. B., 1984. A Kirchhoff method for the computation of finite-frequency body wave synthetic seismograms in laterally inhomogeneous media, *Geophys. J. R. astr. Soc.*, **78**, 413–429.

Fuchs, K., 1971. The method of stationary phase applied to the reflection of spherical waves from transition zones with arbitrary depth dependent elastic moduli and density, *Z. Geophys.*, **37**, 89–117.

Haddon, R. A. W., 1982. Application of Kirchhoff's formula for computation of synthetic seismograms in laterally heterogeneous structures, *Eos, Trans. Am. geophys. Un.*, **63**, 1042.

Haddon, R. A. W., 1983. The Kirchhoff-ray theory method for computation of synthetic seismograms in 2D heterogeneous structures, *Earthq. Notes*, **54**, 78.

Haddon, R. A. W. & Buchen, P. W., 1981. Use of Kirchhoff's formula for body wave calculations in the earth, *Geophys. J. R. astr. Soc.*, **67**, 587–598.

Helmholtz, H., 1860. Theorie der leftschwingungen in Rohren mit offenen enden, *J. reine angew. Math.*, **57**, 1.

Hilterman, F. J., 1970. Three dimensional seismic modeling, *Geophysics*, **35**, 1020–1037.

Hilterman, F. J., 1975. Amplitudes of seismic waves – a quick look, *Geophysics*, **40**, 745–762.

Hilterman, F. J., 1982. Interpretative lessons from three-dimensional modeling, *Geophysics*, **47**, 784–808.

Hilterman, F. J. & Larsen, D. E., 1975. Kirchhoff wave theory for multi-velocity models, *paper presented at 45th annual meeting of the Society of Exploration Geophysics*, Denver, Colorado.

Kanamori, H. & Anderson, D. L., 1977. Importance of physical dispersion in surface wave and free oscillation problems: review, *Rev. Geophys. Space Phys.*, **15**, 105–112.

Karal, F. C. & Keller, J. B., 1959. Elastic wave propagation in homogeneous and inhomogeneous media, *J. acoust. Soc. Am.*, **31**, 694–705.

Kirchhoff, G., 1883. Zur theorie der lichtstrahelen, *Annln Phys.*, **18**, 663.

Love, A. E. H., 1904. The propagation of wave motion in an isotropic elastic solid medium, *Proc. Lond. math. Soc. [2]*, **1**, 291–344.

Love, A. E. H., 1944. *A Treatise on the Mathematical Theory of Elasticity*, Dover, New York.

Maslov, V. P., 1965. *Theory of Perturbations and Asymptotic Methods*, Izd. MGU, Moscow (in Russian). French translation, Dunod, Paris, 1972.

Mow, Chao-Chow & Pao, Yih-Hsing, 1971. The diffraction of elastic waves and dynamic stress concentrations. *Rep. 482-PR*, the Rand Corporation, 1700 Main Street, Santa Monica, California 90406. USA.

Schulman, L. S., 1981. *Techniques and Applications in Path Integration*, Wiley, New York.

Scott, P. & Helmberger, D. H., 1983. Applications of the Kirchhoff-Helmholtz integral to problems in seismology, *Geophys. J. R. astr. Soc.*, **72**, 237–254.

Sen, M. K. & Frazer, L. N., 1983. Modeling reflections from laterally variable multi-layered elastic media, *Eos, Trans. Am. geophys. Un.*, **64**, 772.

Sinton, J. B. & Frazer, L. N., 1981. Using Kirchhoff's method to compute finite-frequency body wave synthetic seismograms in a laterally inhomogeneous medium, *Eos, Trans. Am. geophys. Un.*, **62**, 956.

Sinton, J. B. & Frazer, L. N., 1982. A method for the computation of finite frequency body wave synthetic seismograms in laterally varying media, *Geophys. J. R. astr. Soc.*, **71**, 37–55.

Stephen, R. A., 1984. Finite difference seismograms for laterally varying marine models, *J. geophys. Res.*, in press.

Trorey, A. W., 1970. A simple theory for seismic diffractions, *Geophysics*, **35**, 762–784.

Trorey, A. W., 1977. Diffractions for arbitrary source receiver locations, *Geophysics*, **42**, 1177–1192.

Wheeler, L. T. & Sternberg, E., 1968. Some theorems in classical elastodynamics, *Arch. Rat. Mech. Anal.*, **31**, 51–90.

Zherniak, G. F., 1983. Continuation of wavefields in spatially inhomogeneous media, in *Inverse Problems and Interpretation of Geophysical Observations*, Academy of Science of the USSR, Novosibirsk (in Russian).

Ziolkowski, R. W. & Deschamps, G. A., 1980. The Maslov method and the asymptotic Fourier transform: caustic analysis, *Electro. Lab. Sci. Rep. No. 80-9*, University of Illinois at Urbana-Champaign.

Appendix A

Here we give invariant formulae for calculating the local direction of propagation and the displacement of the scattered waves created by a locally plane wave incident on a smooth boundary. Frequent reference is made to Vol. I of Aki & Richards (1980) and these references are abbreviated as AR. Equations (5.32) on p. 144 of AR are of *SH*-waves and we shall replace the symbol S on their left sides by H. Thus, for example, we write $\dot{H}\dot{H}$ instead of $\dot{S}\dot{S}$. Similarly, equations (5.89), which begin on p. 150 of AR, are of *P*- and *SV*-waves so, when referring to these equations, we use V instead of S and write, for example, $\dot{P}\dot{V}$ instead of $\dot{P}\dot{S}$. As shown in Fig. A1, the smooth surface Σ has unit normal $\hat{\mathbf{n}}$ with material parameters α_+, β_+ and ρ_+ on its $+\hat{\mathbf{n}}$ side and parameters α, β, ρ on its $-\hat{\mathbf{n}}$ side. The surface identity tensor on Σ is $\mathbf{I}_1 = \mathbf{I} - \hat{\mathbf{n}}\hat{\mathbf{n}}$ where $\mathbf{I}$ is the identity tensor for the underlying Euclidean 3-space. The formulae we derive here are for the case of a wave incident on the $-\hat{\mathbf{n}}$ side of Σ

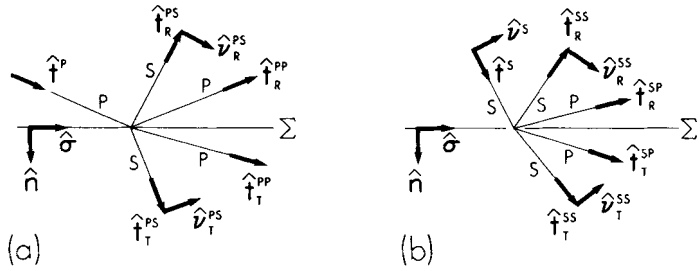

Figure A1. Directions of propagation and directions of displacement for: (a) an incident *P*-wave; and (b) an incident *S*-wave.

Table 1A. Incident *P*-wave. Given quantities are: $\hat{\mathbf{n}}$, the normal to Σ; $\hat{\mathbf{t}}^P$, the direction of propagation of the incident *P*-wave; α, β, ρ, the material parameters on the $-\hat{\mathbf{n}}$ side of Σ_+: α_+, β_+, ρ_+, the material parameters on the $+\hat{\mathbf{n}}$ side of Σ; and $\mathbf{u}^P = A^P\hat{\mathbf{t}}^P$ the displacement of the incident *P*-wave. Derived quantities are $\mathbf{l}_1 = \mathbf{l} - \hat{\mathbf{n}}\hat{\mathbf{n}}$, $\boldsymbol{\sigma} = (\mathbf{t}^P \cdot \mathbf{l}_1)/\alpha$, $\sigma = \|\boldsymbol{\sigma}\|$, and $\hat{\boldsymbol{\sigma}} = \boldsymbol{\sigma}/\sigma$. In the AR formulae $\cos i_1 = \hat{\mathbf{t}}^P \cdot \hat{\mathbf{n}}$, $\cos i_2 = \hat{\mathbf{t}}_T^{PP} \cdot \hat{\mathbf{n}}$, $\cos j_1 = -\hat{\mathbf{t}}_R^{PS} \cdot \hat{\mathbf{n}}$, and $\cos j_2 = \hat{\mathbf{t}}_T^{PS} \cdot \hat{\mathbf{n}}$; and the branch to be taken for each root in column 2 is $\mathrm{Im}(\sqrt{}) \geqslant 0$.

Wave type	Direction of propagation	Displacement
Incident *P*	$\hat{\mathbf{t}}^P$	$\mathbf{u}^P = A^P\hat{\mathbf{t}}^P$
Reflected *P*	$\hat{\mathbf{t}}_R^{PP} = \hat{\mathbf{t}}^P \cdot (\hat{\boldsymbol{\sigma}}\hat{\boldsymbol{\sigma}} - \hat{\mathbf{n}}\hat{\mathbf{n}})$	$\mathbf{u}_R^{PP} = A_R^{PP}\hat{\mathbf{t}}_R^{PP}$
	$= \alpha\sigma\hat{\boldsymbol{\sigma}} - \sqrt{1-\alpha^2\sigma^2}\,\hat{\mathbf{n}}$	$A_R^{PP} = \grave{P}\acute{P}A^P$
Reflected *S*	$\hat{\mathbf{t}}_R^{PS} = \beta\sigma\hat{\boldsymbol{\sigma}} - \sqrt{1-\beta^2\sigma^2}\,\hat{\mathbf{n}}$	$\mathbf{u}_R^{PS} = A_R^{PS}\hat{\mathbf{v}}_R^{PS}$
		$\hat{\mathbf{v}}_R^{PS} = \mathbf{t}_R^{PS} \cdot (\hat{\boldsymbol{\sigma}}\hat{\mathbf{n}} - \hat{\mathbf{n}}\hat{\boldsymbol{\sigma}})$
		$A_R^{PS} = \grave{P}\acute{V}A^P$
Transmitted *P*	$\hat{\mathbf{t}}_T^{PP} = \alpha_+\sigma\,\hat{\boldsymbol{\sigma}} + \sqrt{1-\alpha_+^2\sigma^2}\,\hat{\mathbf{n}}$	$\mathbf{u}_T^{PP} = A_T^{PP}\hat{\mathbf{t}}_T^{PP}$
		$A_T^{PP} = \grave{P}\acute{P}A^P$
Transmitted *S*	$\hat{\mathbf{t}}_T^{PS} = \beta_+\sigma\,\hat{\boldsymbol{\sigma}} + \sqrt{1-\beta_+^2\sigma^2}\,\hat{\mathbf{n}}$	$\mathbf{u}_T^{PS} = A_T^{PS}\hat{\mathbf{v}}_T^{PS}$
		$\hat{\mathbf{v}}_T^{PS} = \hat{\mathbf{t}}_T^{PS} \cdot (\hat{\mathbf{n}}\hat{\boldsymbol{\sigma}} - \hat{\boldsymbol{\sigma}}\hat{\mathbf{n}})$
		$A_T^{PS} = \grave{P}\acute{V}A^P$

as shown in Fig. A1. To use these formulae for a wave incident from $+\hat{\mathbf{n}}$ side one replaces $\hat{\mathbf{n}}$ by $-\hat{\mathbf{n}}$ in each formula containing $\hat{\mathbf{n}}$.

Appendix B

When seismic reflection or refraction data are gathered along a line perpendicular to the strike of the geological structure then these data are often modelled by synthetic seismograms computed using the two-dimensional (2-D) wave equation. In any method of computing synthetics which has a ray theoretical foundation (e.g. geometrical optics, Maslov theory, Gaussian beams, Kirchhoff–Helmholtz) these 2-D solutions are easily converted to approximate 3-D solutions by assuming that the medium has cylindrical symmetry about an axis (generally vertical) through either the source or the receiver. If the departures of the medium from stratification are greatest in the vicinity of the source then it is best to choose this axis through the receiver and vice versa. The switch from one axis to the other can be

Table A2. Incident S-wave. Given quantities are: $\hat{\mathbf{n}}$, the unit normal to Σ; $\hat{\mathbf{t}}^S$, the direction of propagation of the incident S-wave; α, β, ρ, the material parameters on the $-\hat{\mathbf{n}}$ side of Σ; α_+, β_+, ρ_+, the material parameters on the $+\hat{\mathbf{n}}$ side of Σ; and u^S, the displacement of the incident S-wave. Derived quantities are: $\mathbf{I}_1 = \mathbf{I} - \hat{\mathbf{n}}\hat{\mathbf{n}}$, $\boldsymbol{\sigma} = (\hat{\mathbf{t}}^S \cdot \mathbf{I}_1)/\beta$, $\sigma = ||\,\boldsymbol{\sigma}\,||$, $\hat{\boldsymbol{\sigma}} = \boldsymbol{\sigma}/||\,\boldsymbol{\sigma}\,||$, $\boldsymbol{\eta} = \mathbf{u}^S \cdot (\mathbf{I}_1 - \boldsymbol{\sigma}\boldsymbol{\sigma})$, and $\hat{\boldsymbol{\eta}} = \boldsymbol{\eta}/||\,\eta\,||$. In the AR formulae $\cos i_1 = -\hat{\mathbf{t}}_R^{SP} \cdot \hat{\mathbf{n}}$, $\cos i_2 = \hat{\mathbf{t}}_T^{SP} \cdot \hat{\mathbf{n}}$, $\cos j_1 = \hat{\mathbf{t}}^S \cdot \hat{\mathbf{n}}$, and $\cos j_2 = \hat{\mathbf{t}}_T^{SS} \cdot \hat{\mathbf{n}}$; and the branch to be taken for each root in column 2 is $\mathrm{Im}(\surd) \geqslant 0$.

Wave type	Direction of propagation	Displacement
Incident S	$\hat{\mathbf{t}}^S$	$\mathbf{u}^S = A^V \hat{\boldsymbol{\nu}}^S + A^H \hat{\boldsymbol{\eta}}$
		$\hat{\boldsymbol{\nu}}^S = \hat{\mathbf{t}}^S \cdot (\hat{\mathbf{n}}\hat{\boldsymbol{\sigma}} - \hat{\boldsymbol{\sigma}}\hat{\mathbf{n}})$
Reflected P	$\hat{\mathbf{t}}_R^{SP} = \alpha\sigma\hat{\boldsymbol{\sigma}} - \sqrt{1-\alpha^2\sigma^2}\,\hat{\mathbf{n}}$	$\mathbf{u}_R^{SP} = A_R^{SP}\hat{\mathbf{t}}_R^{SP}$
		$A_R^{SP} = \grave{V}\acute{P}A^V$
Reflected S	$\hat{\mathbf{t}}_R^{SS} = \hat{\mathbf{t}}^S \cdot (\hat{\boldsymbol{\sigma}}\hat{\boldsymbol{\sigma}} - \hat{\mathbf{n}}\hat{\mathbf{n}})$	$\mathbf{u}_R^{SS} = A_R^{SV}\hat{\boldsymbol{\nu}}_R^{SS} + A_R^{SH}\hat{\boldsymbol{\eta}}$
	$= \beta\sigma\hat{\boldsymbol{\sigma}} - \sqrt{1-\beta^2\sigma^2}\,\hat{\mathbf{n}}$	$\hat{\boldsymbol{\nu}}_R^{SS} = \hat{\mathbf{t}}_R^{SS} \cdot (\hat{\boldsymbol{\sigma}}\hat{\mathbf{n}} - \hat{\mathbf{n}}\hat{\boldsymbol{\sigma}})$
		$A_R^{SV} = \grave{V}\acute{V}A^V$; $A_R^{SH} = \grave{H}\acute{H}A^H$
Transmitted P	$\hat{\mathbf{t}}_T^{SP} = \alpha_+\sigma\hat{\boldsymbol{\sigma}} + \sqrt{1-\alpha_+^2\sigma^2}\,\hat{\mathbf{n}}$	$\mathbf{u}_T^{SP} = A_T^{SP}\hat{\mathbf{t}}_T^{SP}$
		$A_T^{SP} = VPA^V$
Transmitted S	$\hat{\mathbf{t}}_T^{SS} = \beta_+\sigma\hat{\boldsymbol{\sigma}} + \sqrt{1-\beta_+^2\sigma^2}\,\hat{\mathbf{n}}$	$\mathbf{u}_T^{SS} = A_T^{SV}\hat{\boldsymbol{\nu}}_T^{SS} + A_T^{SH}\hat{\boldsymbol{\eta}}$
		$\hat{\boldsymbol{\nu}}_T^{SS} = \hat{\mathbf{t}}_T^{SS}(\hat{\mathbf{n}}\hat{\boldsymbol{\sigma}} - \hat{\boldsymbol{\sigma}}\hat{\mathbf{n}})$
		$A_T^{SV} = \grave{V}\grave{V}A^V$; $A_T^{SH} = \grave{H}\grave{H}A^H$

made continuously so as to accommodate, for example, deep departures from stratification beneath the source and shallow departures from stratification near the receiver.

Consider first the geometrical optics equations (13) and (14). The spreading factors B^P and B^S are given for 3-D by equations (15) and for 2-D by equations (16). To convert a 2-D solution to a 3-D solution for a P-wave, say, we multiply our 2-D solution by the ratio of (16a) and (15a), i.e. by the conversion factor

$$C_1^P = \frac{\sqrt{8\pi\omega\alpha_1\, dl/d\theta}\,\exp(-i\pi/4)}{4\pi\alpha_1\sqrt{dA/d\Omega}}. \tag{B1}$$

To simplify this relation let $\mathbf{x}(\theta, \phi, T)$ be a point on the wavefront which contains the receiver $\mathbf{x}_2$. Here θ, ϕ are spherical polar coordinates at the source $\mathbf{x}_1$ and θ is the same polar angle which appears in the quantity $dl/d\theta$. On this wavefront let dA be the patch of area that is the cross-section of the ray tube that subtends solid angle $d\Omega = \sin\theta\, d\theta\, d\phi$ at the source. Then assuming the medium is cylindrically symmetric about the polar axis, it follows that $dA = ||\,\partial\mathbf{x}/\partial\theta \times \partial\mathbf{x}/\partial\phi\,||\, d\theta\, d\phi = (dl/d\theta)(d\theta)(x\, d\phi)$ where x is the *horizontal* distance between the source and receiver. Dividing dA by $d\Omega$ we obtain

$$dA/d\Omega = (dl/d\theta)(x/\sin\theta) \tag{B2}$$

and substitution of this quantity into (B1) yields

$$C_1^P = \exp(-i\pi/4)\left(\frac{\omega}{2\pi x}\right)^{1/2}\left(\frac{\sin\theta}{\alpha_1}\right)^{1/2}. \tag{B3}$$

The conversion factor for S-waves is the same except that α_1 is replaced by β_1.

Suppose now that instead of assuming cylindrical symmetry about an axis through the source we assume it holds about an axis through the receiver. We may take advantage of

seismic reciprocity to write formulae analogous to (15), (16) and (17) for our response and then make an argument the same as that just given to find

$$C_2^P = \exp(-i\pi/4)\left(\frac{\omega}{2\pi x}\right)^{1/2}\left(\frac{\sin\theta_2}{\alpha_2}\right)^{1/2} \tag{B4}$$

where θ_2 is the angle which the geometrical ray from $\mathbf{x}_1$ to $\mathbf{x}_2$ makes with the axis of cylindrical symmetry at the receiver. In a stratified medium the axis of symmetry is normal to the stratification and the final factors in (B3) and (B4) are then both equal to ray parameter p. In this case, as expected, $C_1^P = C_2^P \propto (\omega p/2)H_0^{(1)}(\omega p x)/\exp(i\omega p x)$ where $H_0^{(1)}$ is the Hankel function of the first kind of order zero.

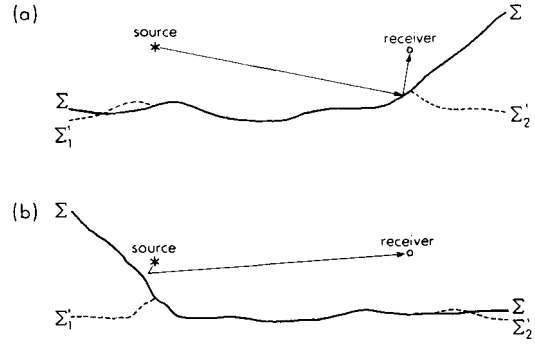

Figure B1. Use of approximate 3-D/2-D conversion factors. The use of C_1^P means a virtual reflector Σ_1' and the use of C_2^P means a virtual profile Σ_2'. (a) Here C_1^P is better than C_2^P; (b) here C_2^P is better than C_1^P.

Although equations (B3) and (B4) were derived using geometrical optics they may be applied to any solution involving a generalized ray which has a well-defined angle with a polar axis at either the source or the receiver. Consider how to apply them to the KH equations (23)–(26). If departures from stratification are greater in the vicinity of the receiver, as shown in Fig. B1(a) then we put C_1^P under the integral sign in (23)–(26). (Note that x in equation (B3) for C_1^P is the horizontal distance from $\mathbf{x}_1$ to $\mathbf{x}_2$, *not* the distance from $\mathbf{x}_1$ to $\mathbf{x} \in \Sigma$.) On the other hand, if departures from stratification are greater in the vicinity of the source, as shown in Fig. B1(b), then C_1^P should be used instead. The examples shown in Fig. B1 are extreme. In general, the integrands of (23)–(26) will contain many arrivals not all of which can be associated with a single neighbourhood. To account for this we suggest the use of an average factor which will act more like C_2^P when $\sin\theta$ is small and act more like C_1^P when $\sin\theta_2$ is small. One example of such a factor is

$$C^P = \exp(-i\pi/4)\left(\frac{\omega}{2\pi x}\right)^{1/2}\left(\frac{\sin\theta\cos\theta_2}{\alpha_1} + \frac{\sin\theta_2\cos\theta}{\alpha_2}\right)^{1/2}. \tag{B5}$$